TECHNICAL NOTES

NATIONAL ADVISORY COMMITTEE FOR AERONAUTICS

No. 613

THE EFFECT OF CURVATURE ON THE TRANSITION FROM LAMINAR TO TURBULENT BOUNDARY LAYER

By Milton Clauser and Francis Clauser
California Institute of Technology

Washington
September 1937

NATIONAL ADVISORY COMMITTEE FOR AERONAUTICS

TECHNICAL NOTE NO. 613

THE EFFECT OF CURVATURE ON THE TRANSITION FROM LAMINAR TO TURBULENT BOUNDARY LAYER

By Milton Clauser and Francis Clauser

SUMMARY

In the flow over the upper surface of a wing, a discrepancy between the predicted and actual point of transition from laminar to turbulent boundary layer had been found. This effect may be due to the comparatively small radius of curvature of the upper surface of the wing. The present tests were undertaken to investigate this effect.

As no available channel was suitable for this work, a new channel with two working sections was built. One working section had a wall with a 20-inch radius of curvature and the other section had a flat wall.

Three types of measurement were made: (a) Traverses were made with a total-head tube to determine the character of the boundary layer at various Reynolds Numbers. (b) The turbulence distribution in the boundary layer was investigated by means of a hot wire and a vacuum-tube amplifier. (c) A similar investigation of the mean velocity distribution in the boundary layer was made by a hot-wire anemometer.

It was found that, by using an abbreviated form of the turbulence-level traverses, critical Reynolds Numbers for the transitions could be established. These critical Reynolds Numbers are plotted as a function of the ratio of the distance of the transition from the leading edge of the plate to the radius of curvature of the plate for both the convex and concave side of the plate. The experimental points for the convex and concave side of the sheet are consistent with each other. The variation is of such an order of magnitude that the curvature ordinarily used on the upper surface of an airplane wing might double the critical Reynolds Number.

INTRODUCTION

In practically every paper on the performance of the modern high-speed airplane, a statement can be found to the effect that, since great strides have been made in "cleaning up" airplanes aerodynamically, the points which once seemed unimportant have recently become the focus of the designer's attention. This statement is exemplified by the interest shown in the skin-friction drag.

It has long been known that for a certain range of Reynolds Numbers the laminar skin-friction coefficient is much smaller than the turbulent skin-friction coefficient for any Reynolds Numbers obtainable in practice. It has also been discovered that the transition from laminar to turbulent boundary layer on the top surface of a wing occurs at a point much farther back on the wing than would be predicted from transition measurements made on a flat plate. The primary cause of this discrepancy was thought to be due to the effect on the boundary layer of the very high curvature of the upper surface of the wing. It was to investigate this point that the present series of tests was instituted.

The authors wish to thank the National Advisory Committee for Aeronautics for its financial assistance in sponsoring the project, Dr. Th. von Kármán and Dr. Clark Millikan for their constant interest and guidance in the experimental program, Dr. A. L. Klein and Dr. E. E. Sechler for their many helpful suggestions on the design of the apparatus, and Mr. A. C. Charters for his help and cooperation while working on the straight section.

DESIGN OF APPARATUS AND EQUIPMENT

When this series of tests was started, the only channel suited for this work was the small one that had previously been used by Wattendorf (reference 1) in determining the effect of curvature on fully developed turbulent flow. This channel has several disadvantages. It operates at subatmospheric pressure, which causes the walls to deflect inward as the speed increases. At the same time, any hole admitting measuring instruments might also admit enough air to seriously disturb the flow. The channel is so small that difficulty has been experienced in using correspond-

ingly small measuring instruments. The final, but perhaps the most important disadvantage, is that the channel is not easily adaptable to starting the boundary layer with zero thickness at the beginning of the curvature.

It was decided to build a new channel to overcome these difficulties. The new tunnel should operate at atmospheric pressure to prevent wall deflections and this feature was accomplished by putting the fan ahead of the working section. (See fig. 1.) A detailed description of the channel is given in Appendix I of this paper. In this arrangement the pressure drop across the fan is approximately equal to the dynamic pressure in the working section (except for friction losses and the expansion at the exit). In order to damp out the turbulence of the fan, a large pressure box (fig. 1) was added between the fan and the working section. In this box were placed two screens comprised of several layers of cheesecloth, which served to damp out the large eddies and give a uniform flow of very fine-scale turbulence that damped out before the air reached the working section. Between the fan and the pressure box was placed a diffuser by means of which some of the kinetic energy of the air was converted into pressure before it entered the box. Undesirable drafts and eddy currents in the room were prevented by another diffuser placed after the working section. Into this diffuser were built two screens to create a pressure drop to counteract the pressure rise of the diffusion.

A great deal of thought was given to the design of the working section. (See Appendix I.) It was desirable to have the channel as large as possible and yet have a favorable aspect ratio to assure two-dimensional flow. The channel was made as tall as the pressure box, which was 7 feet high. A 12:1 aspect ratio was decided upon which made the channel 7 inches wide. In order that the boundary layer start with zero thickness, measurements were made on a sheet suspended midway between the side walls and extending the full height of the channel. This sheet presented both a convex and concave surface of the same radius of curvature. As only the effect of curvature was desired, any pressure gradient in the channel was eliminated by making the side walls adjustable.

The choice of the radius of curvature was more difficult. The theoretical aspects of the problem were first investigated. The amount of curvature may be expressed numerically by the parameter δ/r, where δ is the bound-

ary-layer thickness and r is the radius of curvature of the wall. Since the boundary-layer thickness is a function of the distance x that the flow has traveled along the plate, the ratio x/r may also be used. The critical Reynolds Number R_c of the transition from laminar to turbulent boundary layer on a flat sheet is a constant, other conditions being constant, but for a curved sheet it becomes a function of x/r. The object of this research was to determine the dependence of $R_c = \frac{Ux}{\nu}$ on x/r where U is the mean free-stream velocity and ν is the kinematic viscosity of the air. The method of determination was to make measurements at a point on the sheet, i.e., for a value of x/r, while varying the Reynolds Number by varying the speed U, until the transition was reached. A critical R_c was thus obtained for a value of x/r. Similar measurements were made at other points on the sheet, on both the concave and convex sides. By this method the criticsl Reynolds Numbers were obtained for a series of values of x/r. The object of this discussion is to point out the fact that the effect of curvature on the critical Reynolds Number over a considerable range can be obtained with one radius of curvature. With the aid of a paper by Schlichting (reference 2), it was decided that a central sheet 48 inches long and with a 20-inch radius of curvature would permit the measurement of critical Reynolds Numbers for a sufficiently wide range of values of x/r.

In order to adjust the turbulence level of the free stream and to measure the critical Reynolds Number for no curvature, a straight section similar to the curved one was made. It is also planned to use this section to measure the effect of roughness on the transition.

When the tests were started, the straight section was initially used. The turbulence in the free stream, measured by a hot wire and an amplifier, was found to be very high with frequent "bursts" that made the needle of the amplifier output meter go off the scale. (The details and technique of the hot-wire apparatus are covered in Appendix II.) This difficulty was obviated by putting sheets of plywood across the corners of the pressure box near the exit (fig. 1) where standing vortices were being formed and released into the stream. The result was a fairly steady reading indicating about one-half of 1 percent turbulence in the free stream. All further tests on the straight section were then deferred until the next school year and measurements were begun on the curved section.

MEASUREMENTS ON THE CURVED SECTION

From the results of work done by Dryden (reference 3, fig. 22), it is seen that there is a point of maximum turbulence on the boundary layer near the transition. It was thought that it would be possible to utilize this phenomenon in locating the transition by placing a hot wire in the boundary layer and increasing the velocity until a point of maximum turbulence was reached.

At the beginning of the tests, however, no definite idea could be formed as to where a transition was to be expected, as the effect of curvature was unknown. The optimum distance from the wall to place the hot wire was also unknown. For these reasons it was decided to make total-head surveys at several points for a series of free-stream velocities in order to determine the character of the boundary layer. One set of these surveys is plotted in figure 2. In this figure the ordinates were made dimensionless by dividing by the total pressure of the free stream. These measurements were made before the static pressure was adjusted to zero so that the curves were not converted to velocity profiles. The striking feature of these curves is that the free-stream total pressure is reached at about the same distance from the wall independently of the free-stream velocity. It was expected that the thickness of both the laminar and turbulent boundary layer would decrease with increasing velocity and that the transition boundary layer would rapidly increase in thickness. As was learned later, the transition extends over a considerable region, and it just happens that the combined effects result in a constant boundary-layer thickness in the region investigated. The shapes of the curves, however, serve to indicate a transition from laminar to turbulent boundary layer. Here was the first indication that the transition would be hard to define because of the gradual change from laminar to turbulent flow. These measurements did show the range within which the transition could be expected and the width of the boundary layer.

When the character of the flow had been tentatively established, the pressure gradient in the channel was adjusted to zero, and the static pressure at about one-half inch from the wall was made equal to the atmospheric pressure. This adjustment was made by a tilting multiple manometer connected to small static tubes placed about every 6 inches around the plate. The final pressure variations were less than 1 percent of the dynamic pressure.

With the foregoing data in mind, the output of a hot-wire amplifier was connected to an oscillograph and visual and photographic measurements were made. The oscillographic records are shown in figures 3, 4, 5, and 6. Figure 3 is a record taken in the free stream that indicates a fine-scale turbulence with a fairly uniform level. Figure 4 is a record of the turbulence in the laminar boundary layer. It is hardly turbulence in the usual connotation of the word but is, in reality, comparatively slow variations that give a fairly large and very unsteady reading on the output meter. Figure 5 is a record of the turbulence in the transition boundary layer. It comprises fluctuations similar to those in the laminar layer and also fluctuations similar to those of figure 6, which were made in the definitely turbulent boundary layer. It is practically impossible to read even a highly damped output meter when measurements are being made in the transition region. From figure 5 it is quite easy to see why the transition appears to be so gradual. The flow at the point of transition being just on the verge of instability is markedly affected by any slight external disturbance. The variations in the free-stream turbulence thus cause the point of transition to continually travel back and forth past the wire. This irregularity necessarily means that any measurements which tend to average the readings make the transition appear to extend over a large region. The meter readings for figure 6 were steady when a highly damped output meter was used.

When locating the transition by means of visual observations on the oscillograph, it was found impossible to make measurements that could be reproduced with any degree of accuracy. This difficulty led the authors to attempt to make a series of turbulence profiles for various speeds at several points. These profiles were first taken at a point 100.2 cm from the leading edge on the convex side of the sheet. The variations in Reynolds Number were obtained by changing the speed. These profiles are shown in figure 7, and are later cross-plotted as equal turbulence level contours in figure 12. Next, additional profiles were taken at points 22.9 cm and 38 cm from the leading edge on the concave side of the sheet and are shown in figures 8 and 9. On the concave side of the sheet, these were the only two points at which it was possible to obtain measurements with the velocities available without drilling more holes to admit the hot wire into the tunnel. After these profiles had been made, a great deal of difficulty was encountered with the hot-wire apparatus and, af-

ter spending considerable time, further measurements of turbulence profiles were postponed until a later period.

It is interesting to compare the two turbulence contours (figs. 10 and 11) for the concave side of the sheet with the one for the convex side (fig. 12) and these in turn with the one given by Dryden, which has been replotted in figure 13. All four show a point of maximum turbulence, which may be taken as a characteristic point of the transition. The effect of curvature is to move this point of maximum turbulence closer to the sheet on the concave side and farther away on the convex side. After the transition, the contour lines for the concave side move rapidly in toward the wall while on the convex side the lines appear to be drawn out in the direction of flow. Dryden's contours are not extended far enough to determine the character of this phenomenon for the straight wall. The peculiar swirls (see fig. 12) in the contours for the convex side of the wall are due to the falling off of the profiles after a maximum had been reached and then suddenly rising again in the vicinity of the wall. This second rise was not noted on the concave side of the sheet.

The movement of the transition along the plate as shown by the three sets of contours for the curved section is in the right direction and will be more fully discussed later. Dryden's contours indicate that the transition for his straight wall came at a later point than any of those given by the curved-section curves. Three factors may have caused this discrepancy: intensity of turbulence, scale of turbulence in the free stream, and surface roughness of the sheet. The level of turbulence in Dryden's tunnel was given as 0.5 percent, which is comparable to that in the curved-wall tunnel. The scale of turbulence in the curved-wall tunnel is unknown, as no velocity correlations have yet been made, and no value was given for Dryden's tunnel. Where Dryden used a polished aluminum sheet, the authors used a rolled and polished steel sheet with numerous small pits, evidently caused by the rolling. More data on the effect of this roughness will be available when the contemplated roughness tests in the straight section are completed.

After the trouble with the hot-wire apparatus developed, it was decided to investigate the possibility of establishing the transition by a series of equal velocity contours similar to the equal turbulence contours. The velocities were measured by a hot-wire anemometer that

permitted measurements very close to the wall. A check run was made, using a total-head tube, and applying the wall correction obtained by Jones (reference 4). The results of both methods are shown in figure 14 for a point of 100 cm from the leading edge and at a speed of 18.5 meters per second. It was decided that the difference was too small to warrant further investigation at this time. More complete profiles are shown in figures 15 to 21. These profiles were cross-plotted as equal velocity contours in figures 22 to 26. Unfortunately, there is no characteristic feature of these contours that can be used in definitely defining a transition.

The hot-wire apparatus had now been restored to working order but insufficient time remained to complete the turbulence contours. When the contours already completed were examined, however, it was a comparatively easy matter to locate the maximum points. The operating technique was as follows: From the turbulence profiles already taken, the distance from the wall at which the point of maximum turbulence would occur could be estimated. With the hot wire in this position, the speed was increased, both the x- and y-Reynolds Numbers proportionately corresponding to a traverse along a line through the origin of a diagram similar to figures 10 to 13. As the speed was increased, a maximum value of turbulence was observed. The wire was then moved in and out until another maximum was observed with the wire in the new position, and the first operation was again repeated. This process is rapidly convergent, the final maximum being usually located at the end of the second trial. The final results are shown in figure 27. These curves were obtained by making turbulence readings at a series of velocities with the hot wire in the final position.

Before a discussion of these results is given, it is perhaps best to see what the effect of curvature might be expected to be. In order to do this, the equation of motion for curved potential flow is written

$$\frac{\partial p}{\partial r} = \rho \frac{u^2}{r} - \rho \frac{u}{r} \frac{\partial v}{\partial \theta}$$

where p is the local pressure.

u, local velocity in surface direction.

v, local velocity in normal direction.

ρ, air density.

r and θ, polar coordinates.

For our case the second term may be considered to be zero:

$$\frac{\partial p}{\partial r} = \rho \frac{u^2}{r}$$

which means that the centrifugal force $\rho \frac{u^2}{r}$ just balances the radial pressure gradient.

Since the vorticity is zero, $\frac{d(ur)}{dr} = 0$. The following sketch shows this velocity distribution and the velocity distributions on both sides of the sheet in the region of the boundary layer.

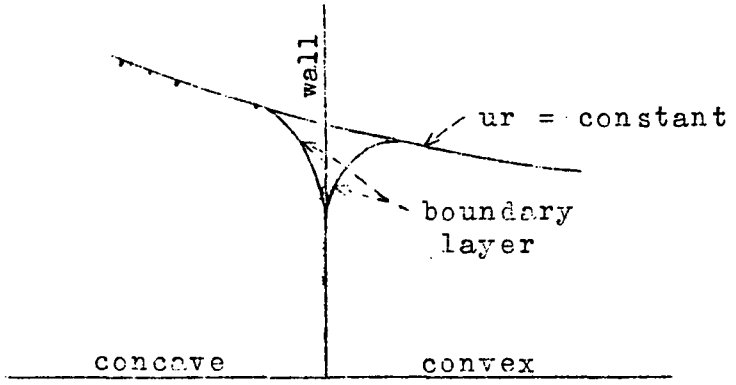

On the concave side of the sheet $\frac{d}{dr}(ur) < 0$ and on the convex side $\frac{d}{dr}(ur) > 0$. First, consider what happens to a particle on the concave side when it is displaced from its path. If it is displaced outward (i.e., into the boundary layer) it will have a velocity $u = \frac{u_o r_o}{r}$ greater than that of its surroundings. This result means that the centrifugal force $\rho \frac{u^2}{r}$ is greater on this particle than on the surrounding particles, and hence the particle is thrown farther outward. Similarly, if the particle is displaced inward. If a particle on the convex side of the

sheet is displaced outward, it has a lower velocity and consequently a lower centrifugal force acting on it than the surrounding particles. Thus it tends to go back to its original position. A similar thing would happen if it were displaced inward. Consequently, disturbances on the concave side of the sheet tend to be amplified and disturbances on the convex side tend to be damped out.

This result leads to the conclusion that the effect of curvature will be to precipitate the transition at an earlier point on the concave side and to prolong it to a later point on the convex side. Figure 27 shows that this effect is exactly what happens. For the concave side of the sheet, the maximum point of the turbulence curves is shifted to the left for increasing values of x/r, and for the convex side the curves are shifted to the right for increasing values of x/r. The experimental points for $\frac{x}{r} = 2.250$ and $\frac{x}{r} = 1.975$ are quite scattered and appear to lie on the same curve. The scatter is due to the low speeds at which it is necessary to run these tests. At these speeds all frequencies are correspondingly lower, which results in a very unsteady reading on the output meter. If it were possible to get an even more highly damped meter, more accurate results might be obtained which should show a separation of these curves.

As was mentioned previously, the turbulence drops off rapidly after the transition is reached on the concave side but is maintained for some distance on the convex side. Thus, there is likely to be some ambiguity in defining a transition. Two definitions have been taken, one being the point where the maximum turbulence is first reached and the other where the turbulence is 95 percent of its maximum value. The first definition is rather indefinite for points on the convex side, as here the maximum is reached rather slowly. The second definition is more concise, as it comes at about the place where the curves start to level off.

Using both definitions, critical Reynolds Numbers have been plotted as a function of x/r in figure 28. In the absence of any further information, two straight lines have been faired through the points. The two sets of points for the two sides of the sheet are surprisingly consistent and lie remarkably close to the faired straight line. It can be seen from the curve that the critical Reynolds Number for a straight sheet turns out to be about

4×10^5. This value agrees approximately with results obtained by van der Hegge Zijnen (R_x = 300,000, reference 5) but is lower than the values obtained by Dryden (R_x = 1,100,000). Some of the possible causes for disagreement with Dryden's work were discussed earlier in the paper. When the straight section of the present tunnel is installed, more data will be available on this point.

Up to the present, the largest portion of the time has been spent on designing and building the apparatus and investigating the different methods of technique and procedure. It is felt that this time has been well spent. It has resulted in developing the first pressure-box type of tunnel to have a very low level of turbulence in the working section. With this type of tunnel, all measurements are made at atmospheric pressure, and no trouble with wall deflections is experienced. In addition, a large variety of knowledge about the behavior of the boundary layer has been obtained. As in all research work, a great many difficulties were encountered; for the most part these have been successfully overcome, and it is hoped that the work in the future will proceed with a minimum of trouble and delay.

The present design of the channel admits of a great variety of boundary layer and transition experiments. It is hoped that the experiments to determine the effect of turbulence and roughness on the transition will be completed within the next year.

CONCLUSIONS

As far as the authors know, the present experimental investigation is the first to show that curvature has a pronounced effect on the transition of the boundary layer from the laminar to the turbulent state.

It appears that three important results have been obtained thus far. First, the experimental points for the convex and concave side of the sheet are consistent with each other and, with the experimental accuracy involved, lie on the same curve. Second, this curve can be approximated by a straight line. Third, the order of magnitude of the variation is such that the curvature ordinarily

used on the upper surface of an airplane wing might double the critical Reynolds Number.

Guggenheim Aeronautics Laboratory,
California Institute of Technology,
Pasadena, California, June 1937.

APPENDIX I

DETAILED DESCRIPTION OF THE VARIOUS PARTS OF THE CHANNEL

Fan

The fan (figs. 29 and 30) was designed with the aid of a report by Keller (reference 6). It has eight wooden blades, mounted adjustably in a steel hub, and is driven by means of two V-belts from a 12½ horsepower direct-current motor. The hub fairing was extended out in front of the tunnel about 2 feet to save making an expensive hub fairing. A counter propeller consisting of eight sheet-metal blades (not shown in the photographs), placed in front of the propeller, serves to eliminate the rotary component of velocity induced by the propeller. At a maximum of 1,500 r.p.m., the fan was designed to give a velocity of from 80 to 90 feet per second in the working section. Velocities as high as 83 feet per second have been obtained.

Diffuser

The diffuser (figs. 31 and 32) consists of an external truncated cone and an inner cylinder that serves as an extension for the fan hub. This arrangement was chosen when it proved to be the cheapest of three different designs. It has an expansion ratio of 2½:1. Thus 84 percent of the dynamic head is converted into static pressure before entering the box.

Pressure Box

The framework of the box is made of 2- by 2-inch angles and I beams. The covering consists of sheets of

1-inch plywood, bolted on and sealed with red lead to prevent leaks. All three of its dimensions are 7 feet. An extensive series of tests was undertaken to make the turbulence level at the exit of the box a minimum. The final arrangement consists of two screens to damp out the eddies of the propeller, and plywood fairings across the corners near the exit. (See fig. 1.) One of the screens was made of two layers of cheesecloth and one layer of copper window screening; the other was made of five layers of cheesecloth. These screens seemed to give a very uniform steady flow across the whole cross section of the box. The plywood fairings served to eliminate standing vortices in the corners of the box.

Working Section

The straight and curved working sections (figs. 33 and 34) are easily interchangeable. The main part of each section is the central 20-gage polished-steel sheet, which is clamped between 2- by 3-inch angles at the ends. These angles are bolted to the external framework (see fig. 35) in such a way as to put up to 100 pounds per inch tension into the sheet, in order to hold it in shape and keep it from vibrating. The side walls were stiffened with vertical 1- by 1-inch angles connected at the top and bottom to the 2- by 3-inch angles by threaded 3/8-inch studs. The distance between the side walls and the center sheet was adjusted by means of the studs, which moved the stiffeners in or out. The leading edge of the central sheet was sharpened with a taper that extended back about 1 inch.

Measuring apparatus, such as pitot tubes and hot wires, were admitted through holes in the outer walls and extended across to the central wall. These instruments were mounted on a micrometer screw carriage on a separate stand. (See fig. 36.)

Exit Diffuser

The exit diffuser (fig. 37) was added to reduce the exit velocity of the air to a point where it would not create undesirable eddies in the surrounding room. In order to overcome the pressure rise due to the divergence, two screens were placed in the diffuser. These screens were adjusted until approximately atmospheric pressure was obtained. The final adjustment was made by shutters at the opening.

APPENDIX II

HOT-WIRE APPARATUS AND TECHNIQUE

Preparing the Hot Wires

The hot wires are made of 0.001-inch Wollaston wire, which is a 0.0001-inch platinum wire with a 0.0009-inch silver covering. The wire was soft-soldered to the holder. In the use of plain platinum wire, trouble had been experienced with poor connections when soft solder was used, but the silver coating on the Wollaston wire gave a very good bond. After the wire was soldered in place, about a half or three-quarters of a millimeter of silver in the center was etched off by means of a bubble of concentrated nitric acid formed at the end of a capillary tube.

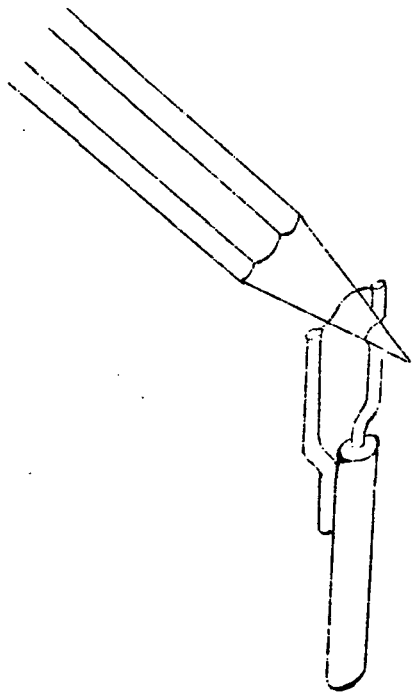

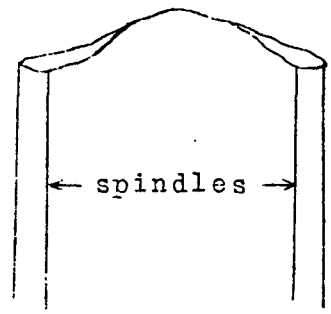

A few valuable points of technique were discovered in soldering the wires. Best results were obtained in both the soldering and etching processes if the wire and spindles were kept as clean as possible. It sometimes took as long as an hour for the acid to eat through a thin film of grease on the wire. While soldering, the spindles were sprung slightly apart so that when released the wire

would have a slight curvature to give it flexibility. Immediately after releasing the spindle the wire bent sharply in the middle. This sharp bend was removed by letting the wire carry the entire weight of the spindles and support on the end of a pencil. When the wire had a very gentle bow in it, the spindles were gently heated with a soldering iron to relieve any residual stresses in the wire. These stresses after etching were sometimes transferred to the etched portion, causing it to take all kinds of queer shapes. If the finished wire has the shape shown in the sketch (p. 14), it will stand a lot of comparatively hard usage.

Operation of the Amplifier

The amplifier (fig. 38) is of standard design. (For diagram of the circuit, see fig. 39.) The four stages, with resistance coupling between stages, give a total gain of about 240,000. The gain is maintained at a constant value by an attenuator and a standard input voltage. Owing to insufficient coupling, the amplifier falls off in gain very rapidly below 100 cycles per second. Above 100 cycles, the increase in gain with frequency proved to be just about sufficient to compensate for the distorted frequency response of the very fine Wollaston wire, which normally requires only a very small amount of compensation. The amplifier had originally been built with a variable unit to compensate a plain platinum wire which, because of its larger diameter, needs a much higher degree of compensation. For this reason a low enough value could not be obtained exactly to compensate the Wollaston wire. Consequently these tests were run without any frequency compensation other than that given automatically by the amplifier.

Method of Calibrating Hot Wires

Two calibrations are necessary for a hot wire; the first is the calibration of the resistance against the mean velocity when the wire is used as an anemometer, and the second is the calibration of the reading of the output meter of the amplifier against the fluctuating velocity at the wire when it is used to measure the level of turbulence. The first calibration is comparatively simple. The resistance of the wire is measured by a Wheatstone bridge at a series of known velocities and a curve is faired through

the experimental points. A typical curve is given in figure 40.

A special tunnel has been designed and built by F. D. Knoblock of the Guggenheim Aeronautics Laboratory at California Institute of Technology for the turbulence calibrations. (See fig. 41.) In this tunnel, the hot wire and holder are vibrated by means of a taut three-wire suspension. The calibration really gives the output reading corresponding to a calculable level of (artificial) turbulence whose amplitude has the form $\Delta = \frac{\Delta_0}{2} \sin 2\pi \omega t$ where Δ_0 is the double amplitude and ω is the frequency. More details of the tunnel will later be published by the designer.

REFERENCES

1. Wattendorf, F. L.: A Study of the Effect of Curvature on Fully Developed Turbulent Flow. Proc. Roy. Soc. (London), series A, vol. 148, no. 865, Feb. 1935, pp. 565-598.

2. Schlichting, H.: Über die Entstehung der Turbulenz in einem Rotierenden Zylinder. Göttingen Nachrichten, Heft 2, 1932, S. 160.

3. Dryden, Hugh L.: Air Flow in the Boundary Layer Near a Plate. T.R. No. 562, N.A.C.A., 1936.

4. The Cambridge University Aeronautics Laboratory: The Measurement of Profile Drag by the Pitot-Traverse Method. R. & M. No. 1688, British A.R.C., 1936.

5. van der Hegge Zijnen, B. G.: Measurements of the Velocity Distribution in the Boundary Layer along a Plane Surface. Report 6, Aero. Lab., Technical High School, Delft, 1924.

6. Keller, C.: Axialgebläse vom Standpunkt der Tragflügeltheorie. Mitteilung aus dem Institute für Aerodynamik, Eidgenossische Technische Hochschule, Zurich, 1934.

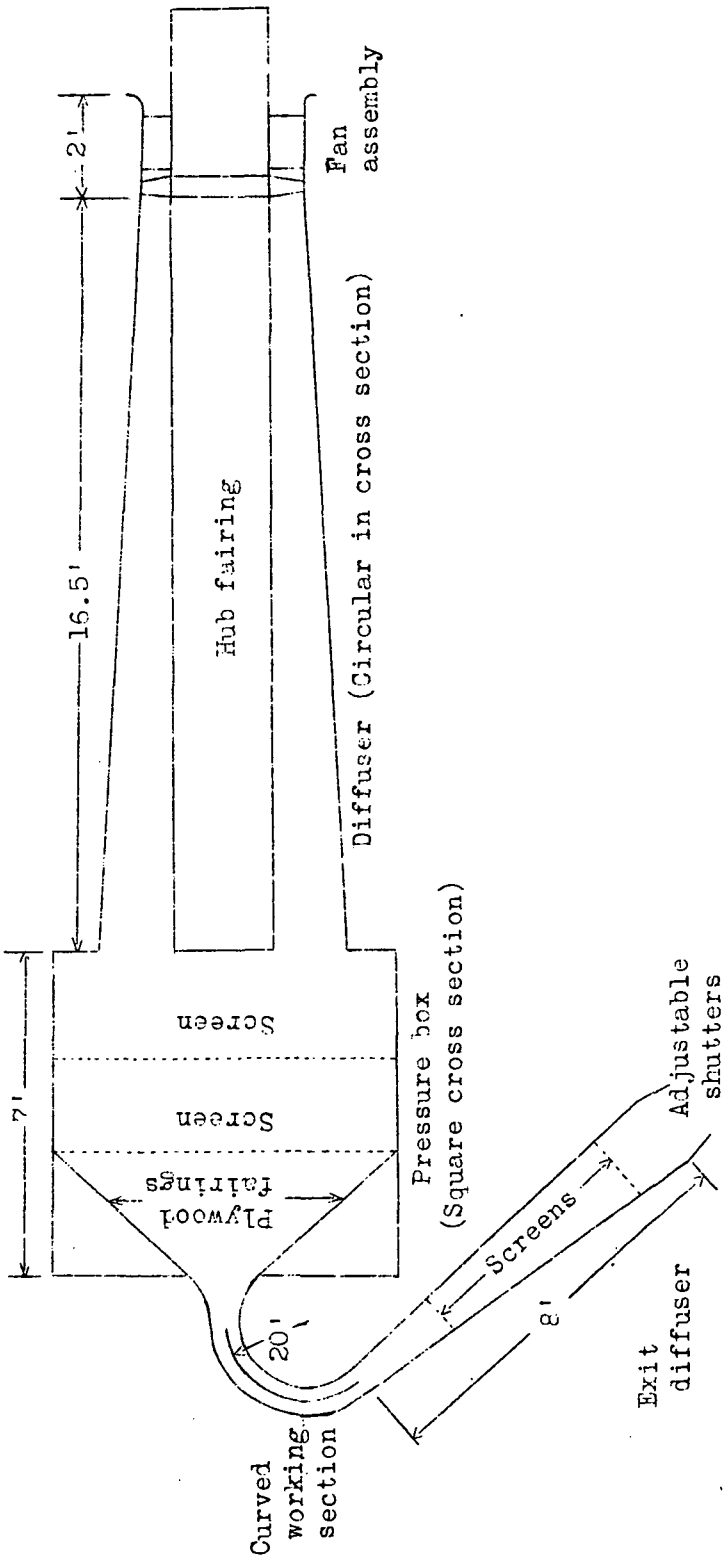

Figure 1.- Diagrammatic sketch of tunnel assembly plan view.

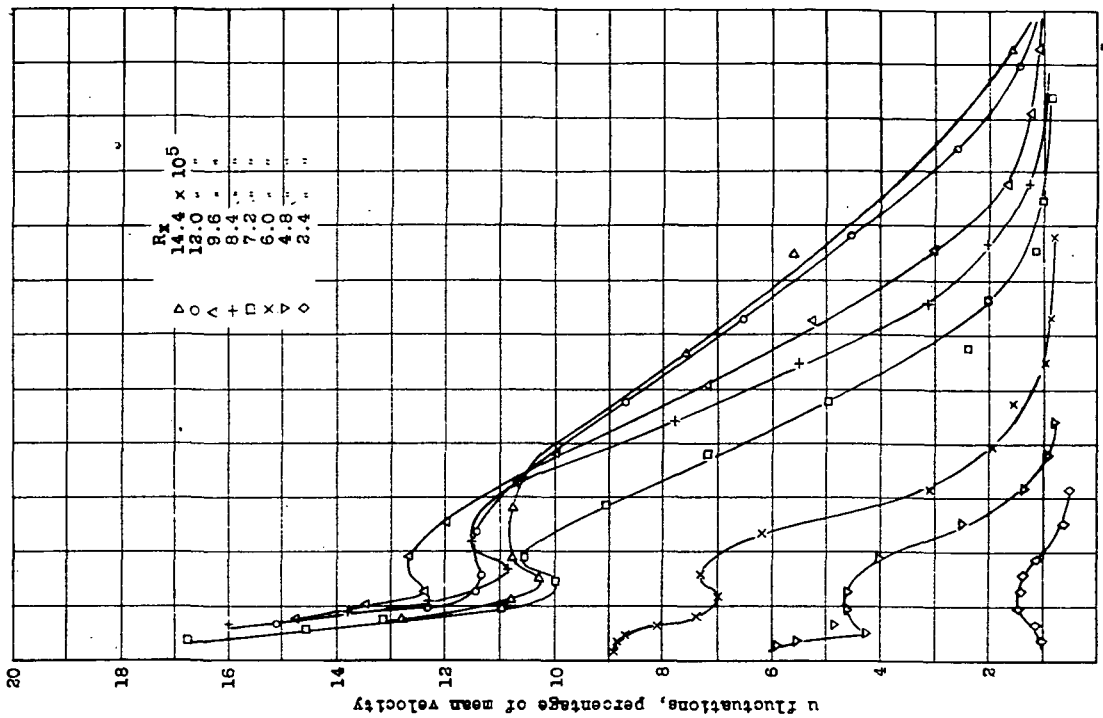

Figure 7.- Turbulence level profiles at x/r = 1.975 on the convex side of the sheet.

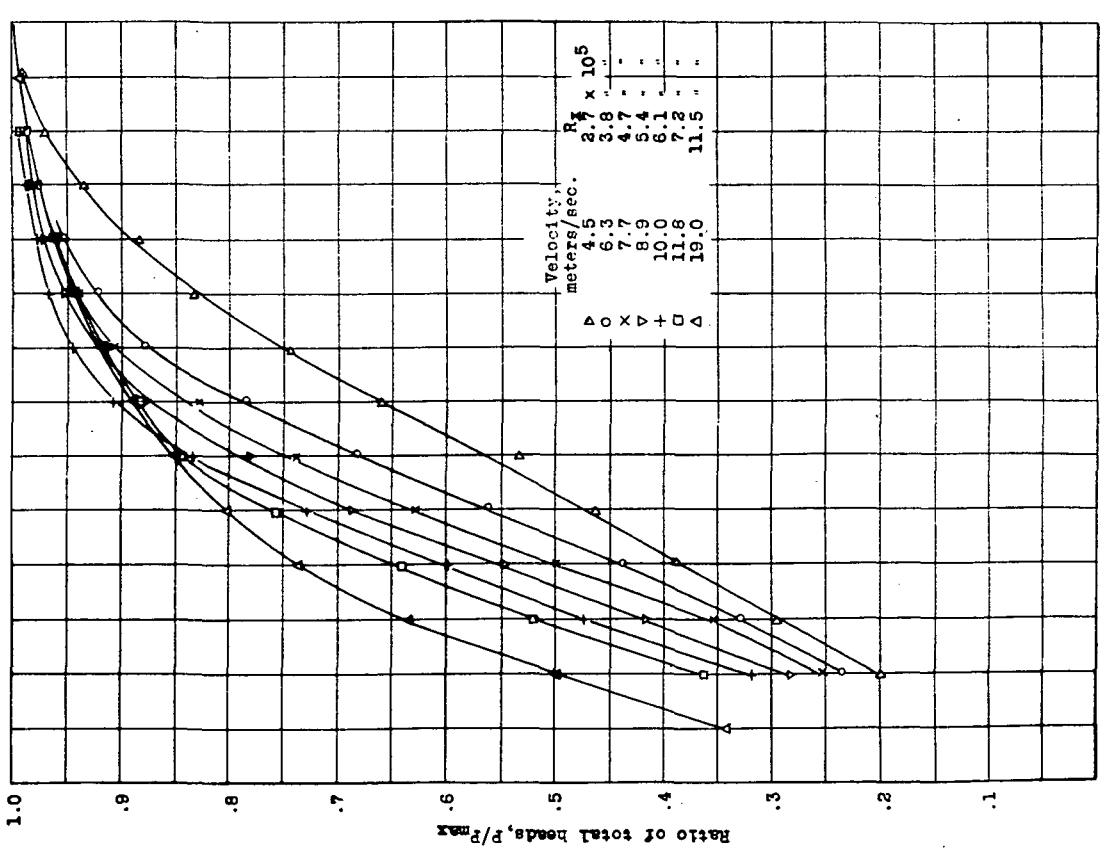

Figure 8.- Total-head traverses at x/r = 1.91 on convex side for various velocities.

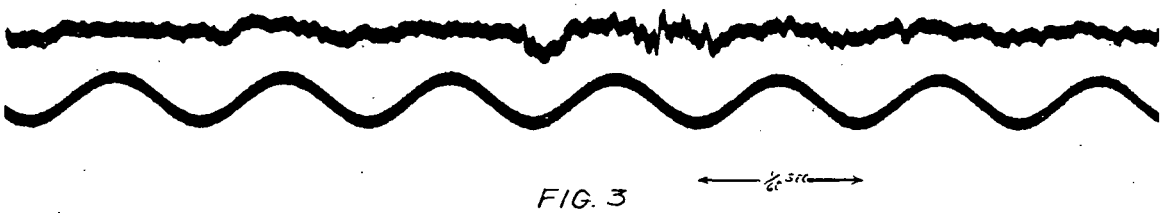

FIG. 3
OSCILLOGRAPHIC RECORD OF TURBULENCE IN THE FREE STREAM.

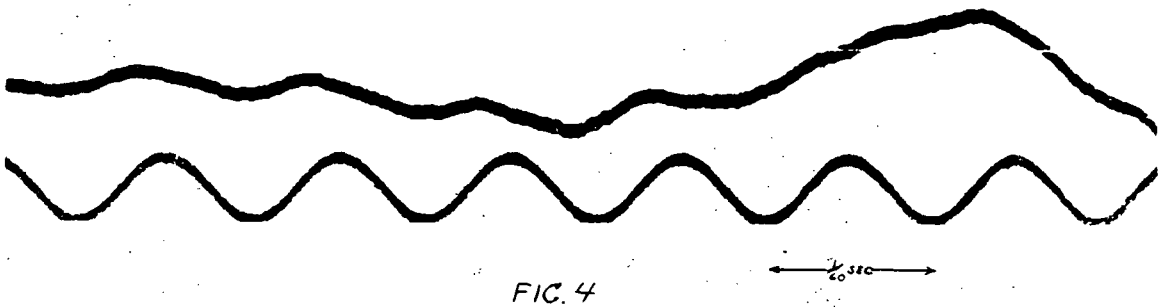

FIG. 4
OSCILLOGRAPHIC RECORD OF TURBULENCE IN LAMINAR BOUNDARY LAYER.

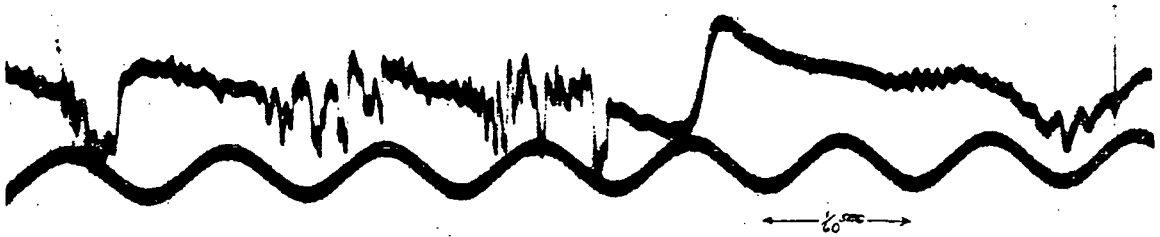

FIG. 5
OSCILLOGRAPHIC RECORD OF TURBULENCE IN TRANSITION BOUNDARY LAYER.

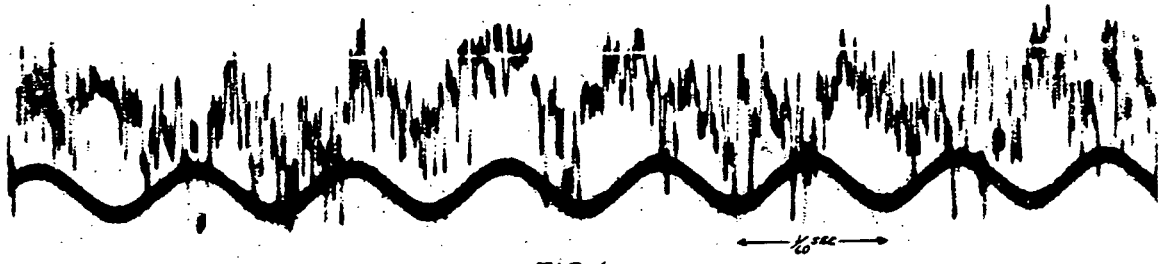

FIG. 6
OSCILLOGRAPHIC RECORD OF TURBULENCE IN TURBULENT BOUND LAYER.

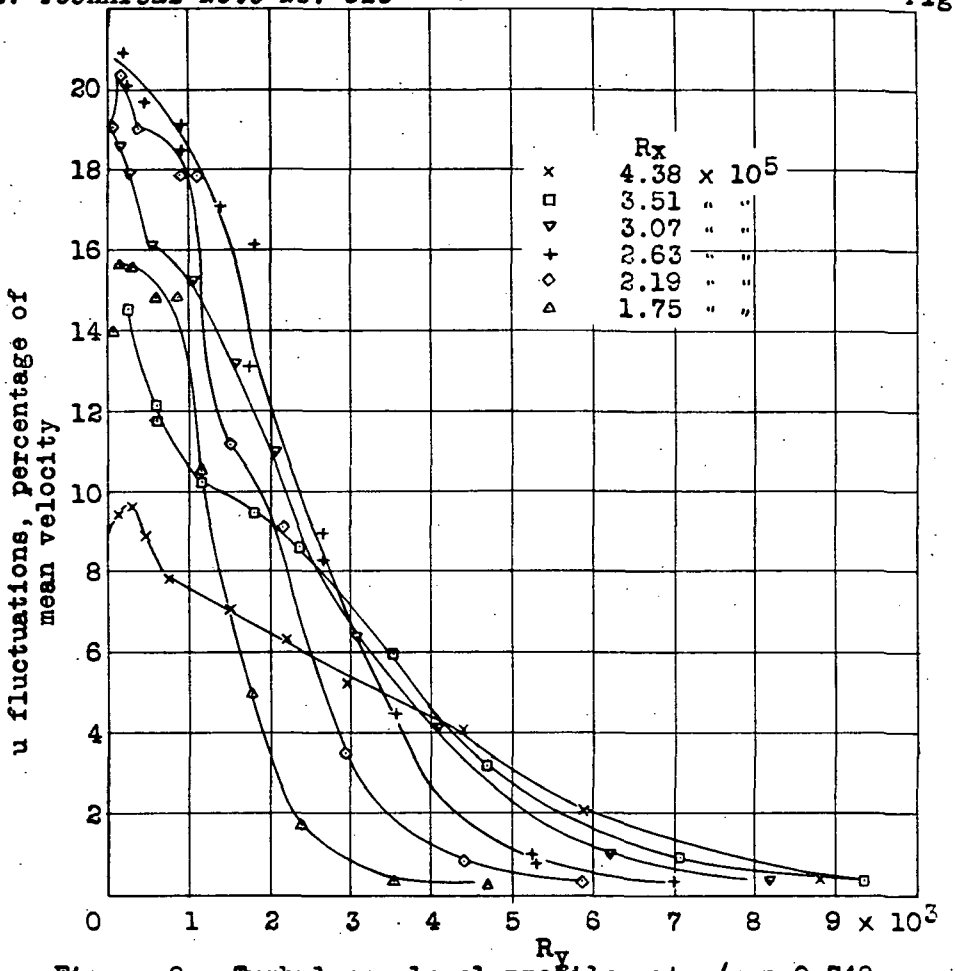

Figure 8.- Turbulence level profiles at x/r = 0.748 on the concave side of the sheet.

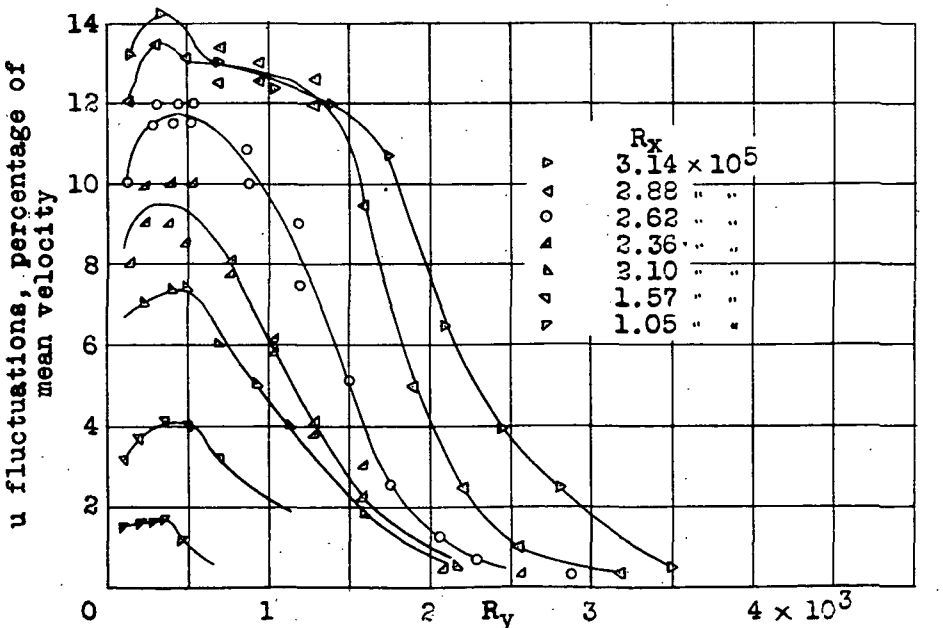

Figure 9.- Turbulence level profiles at x/r = 0.451 on the concave side of the sheet.

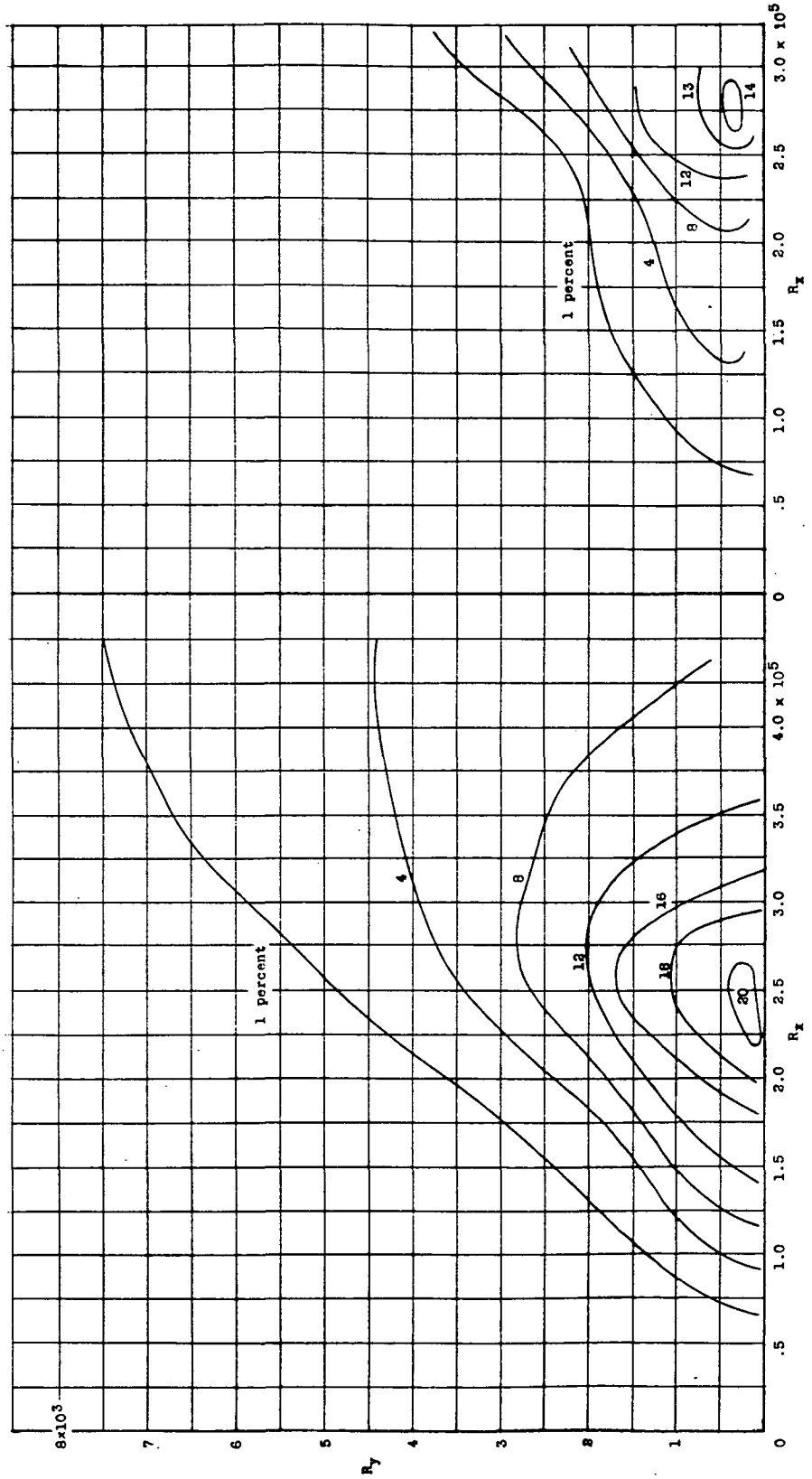

Figure 10.- Equal turbulence level contours at x/r = 0.748 on the concave side of the sheet. The contours give the u fluctuations as percentages of the mean velocity. Cross plot of figure 8.

Figure 11.- Equal turbulence level contours at x/r = 0.481 on the concave side of the sheet. The contours give the u fluctuations as percentages of the mean velocity. Cross plot of figure 9.

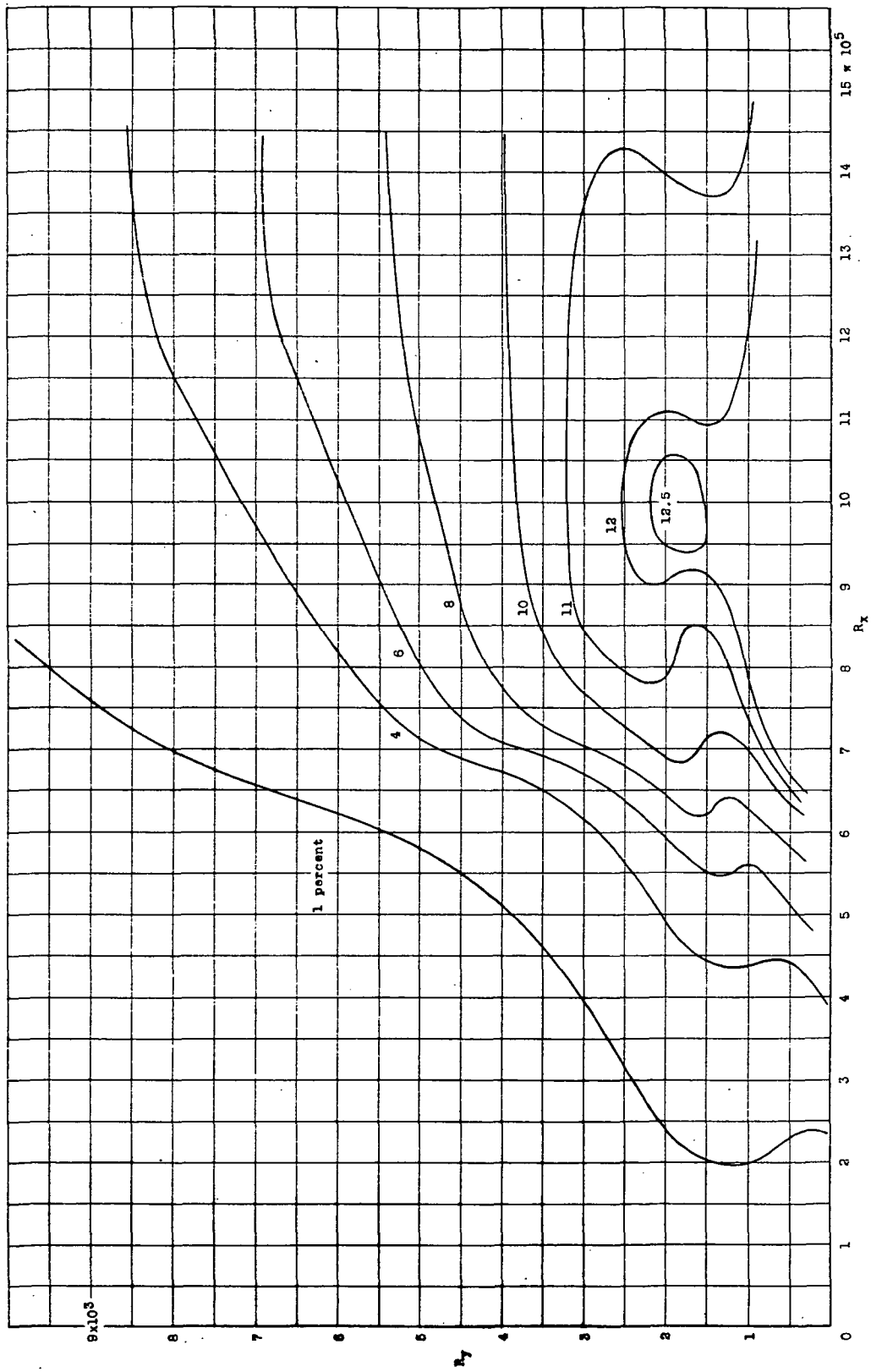

Figure 12.- Equal turbulence level contours at x/r = 1.975 on the convex side of the sheet. The contours give the u fluctuations as percentages of the mean velocity. Cross plot of figure 7.

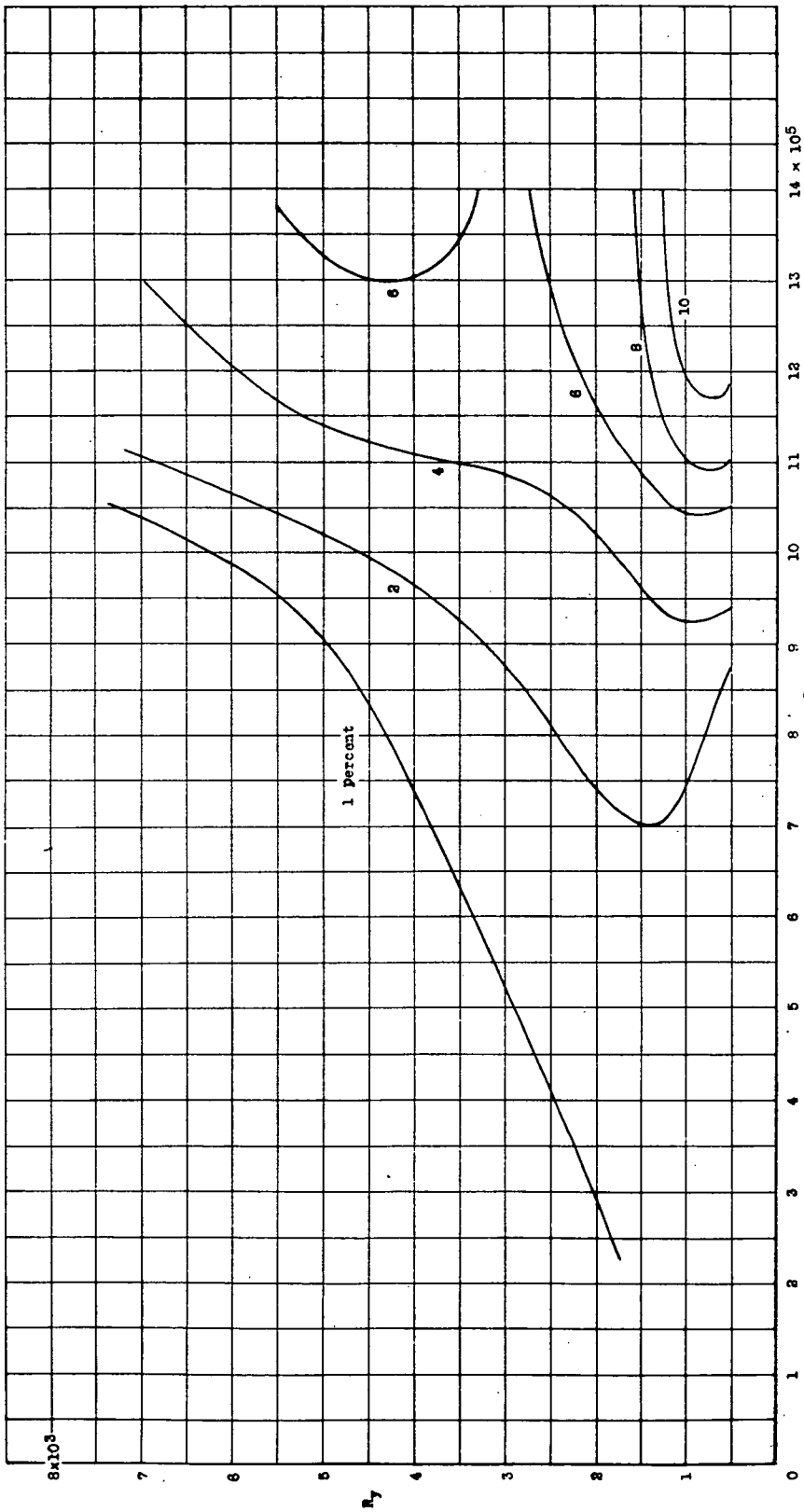

Figure 13.- Equal turbulence level contours for a flat plate. The contours give the u fluctuations as percentages of the mean velocity. Taken from reference 3, figure 22.

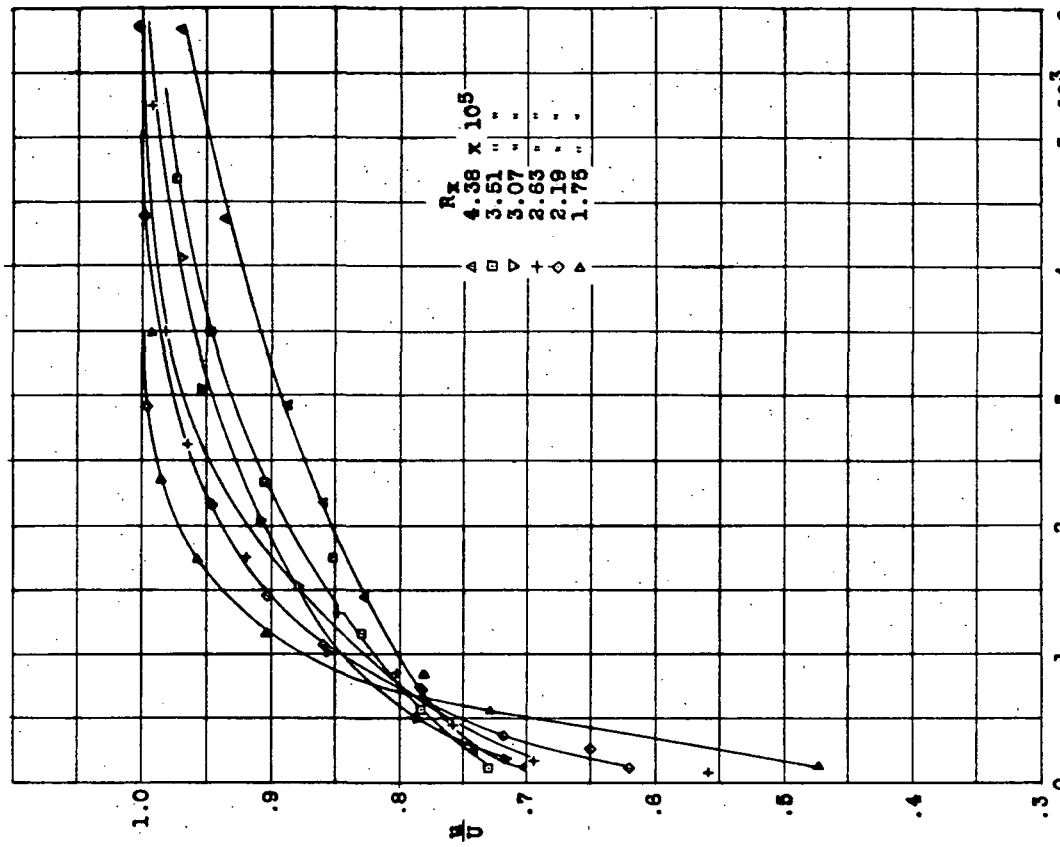

Figure 15.- Mean velocity profiles at x/r = 0.498 on the concave side of the sheet.

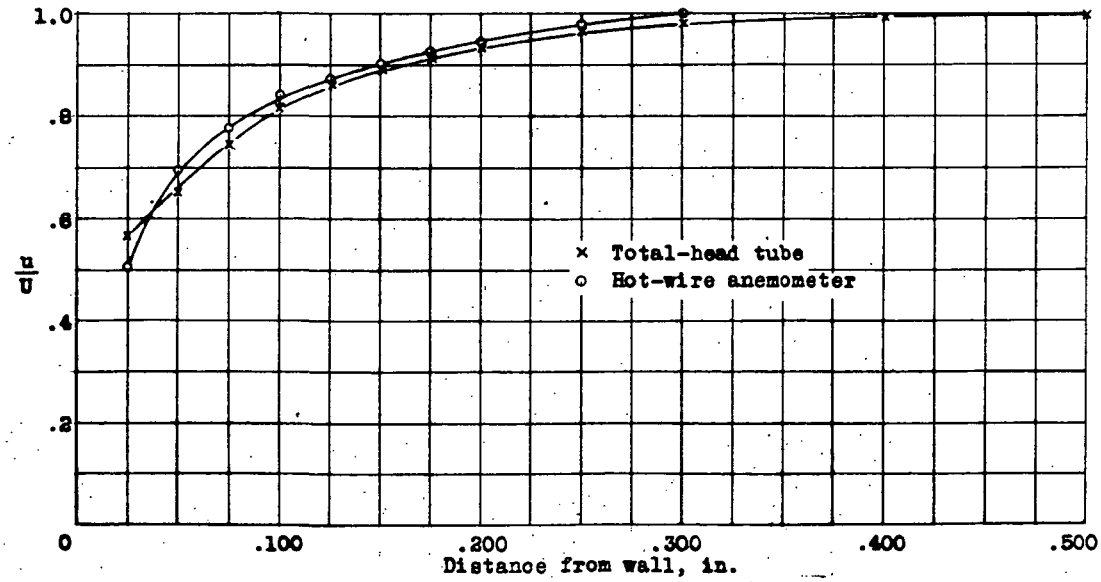

Figure 14.- Comparison of velocity traverses taken with total-head tube and hot-wire anemometer.

Figs. 16,17,18

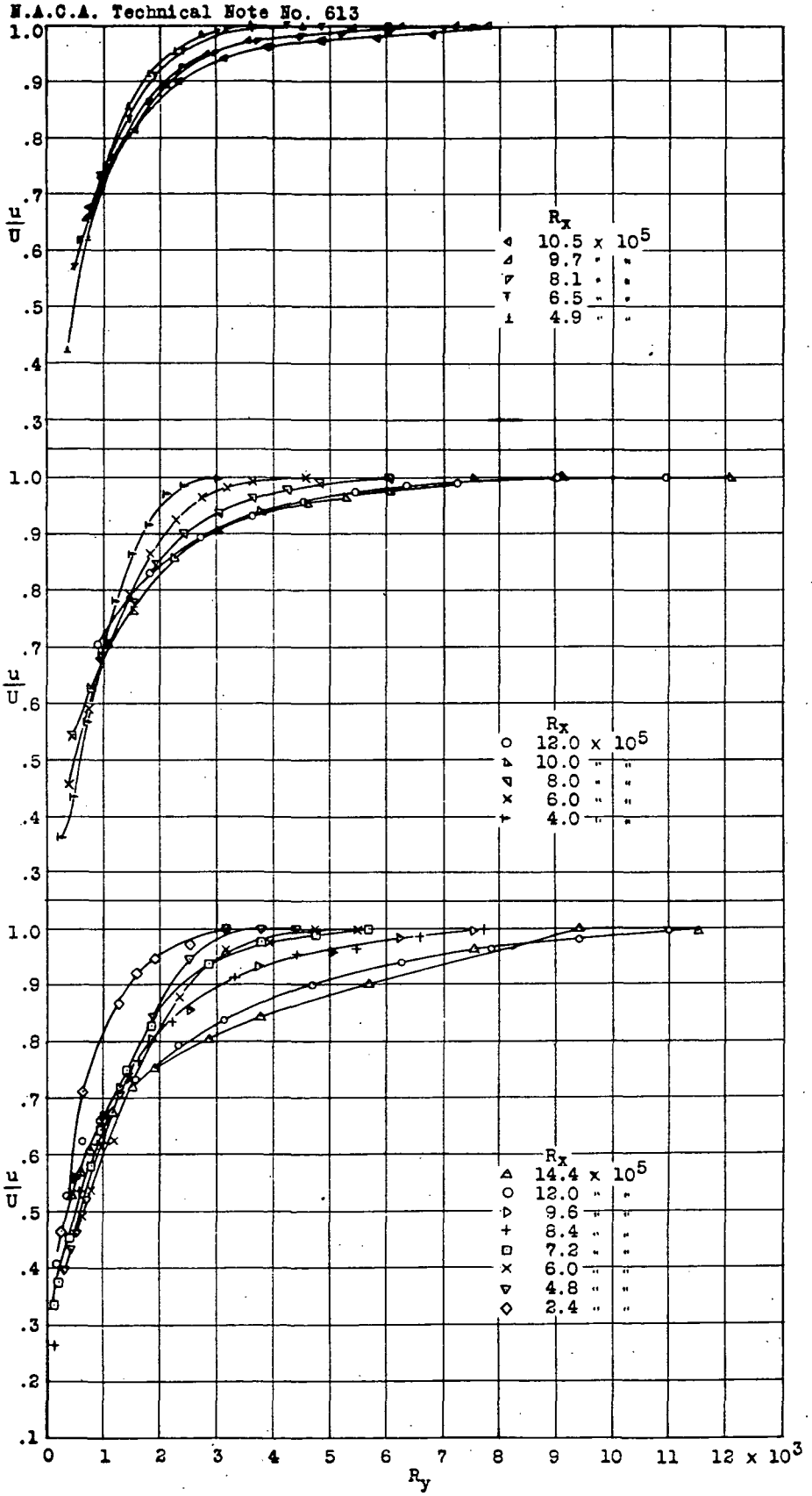

Figure 16.-

Mean velocity profiles at x/r = 1.348 on the convex side of the sheet.

Figure 17.-

Mean velocity profiles at x/r = 1.652 on the convex side of the sheet.

Figure 18.-

Mean velocity profiles at x/r = 1.975 on the convex side of the sheet.
Run 2.

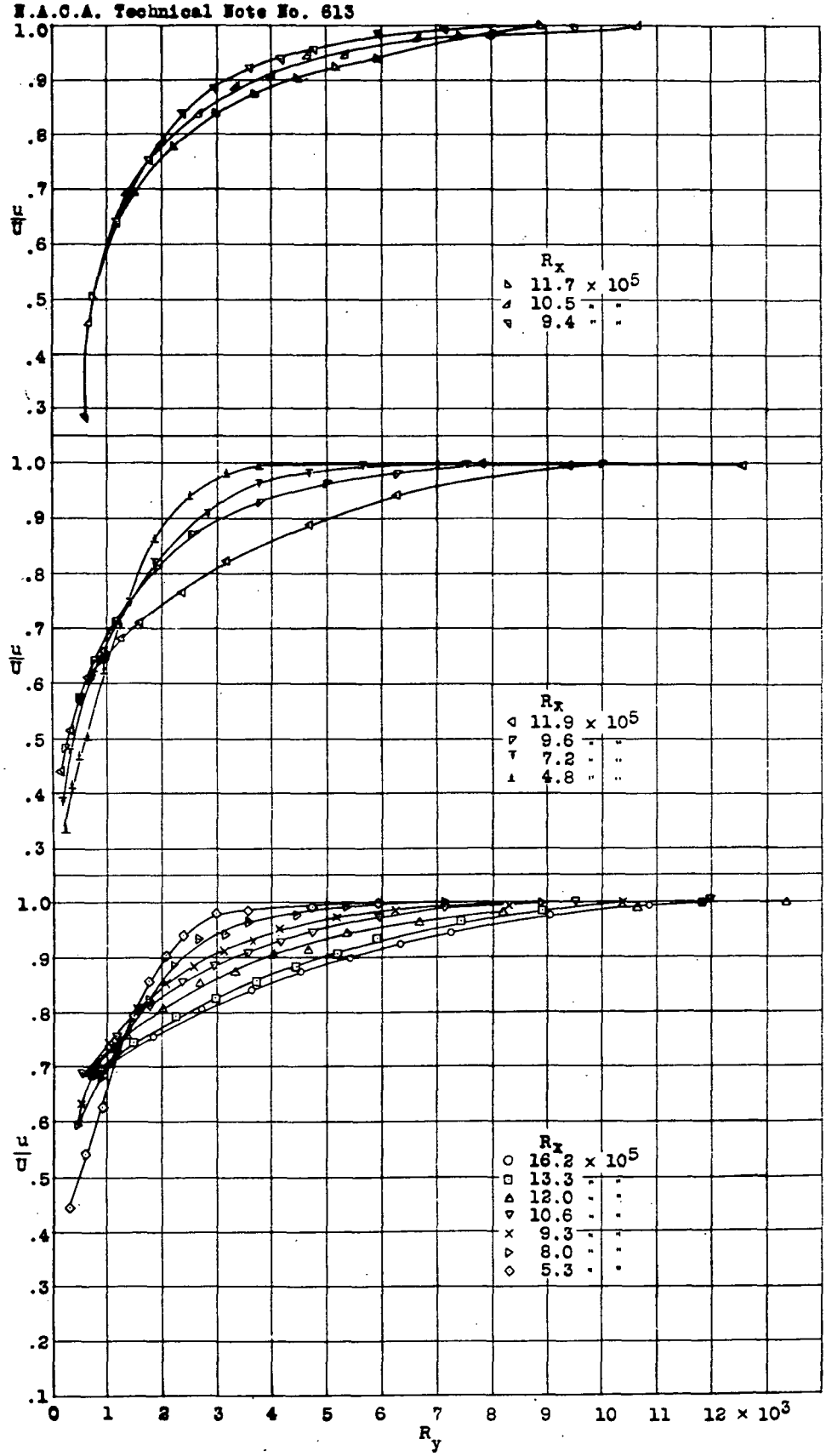

Figure 19.-

Mean velocity profiles at x/r = 1.975 on the convex side of the sheet. Run 9.

Figure 20.-

Mean velocity profiles at x/r = 1.975 on the convex side of the sheet. Run 7.

Figure 21.-

Mean velocity profiles at x/r = 2.250 on the convex side of the sheet.

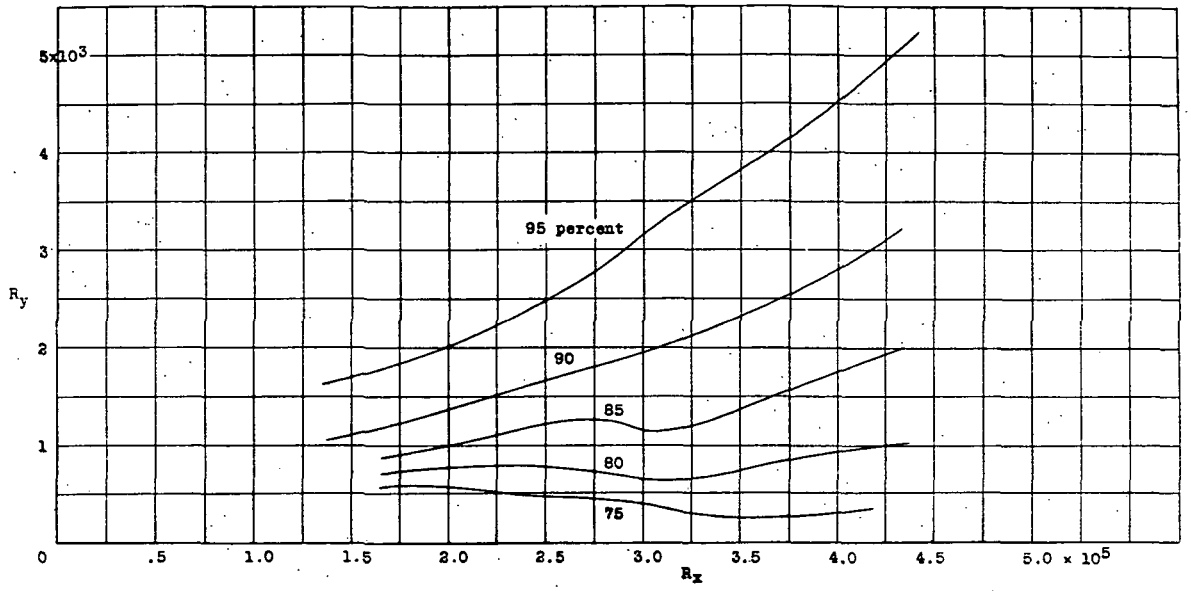

Figure 22.- Equal velocity contours at x/r = 0.748 on the concave side of the sheet. The contours give the mean velocities as percentages of the mean free-stream velocity. Cross plot of figure 15.

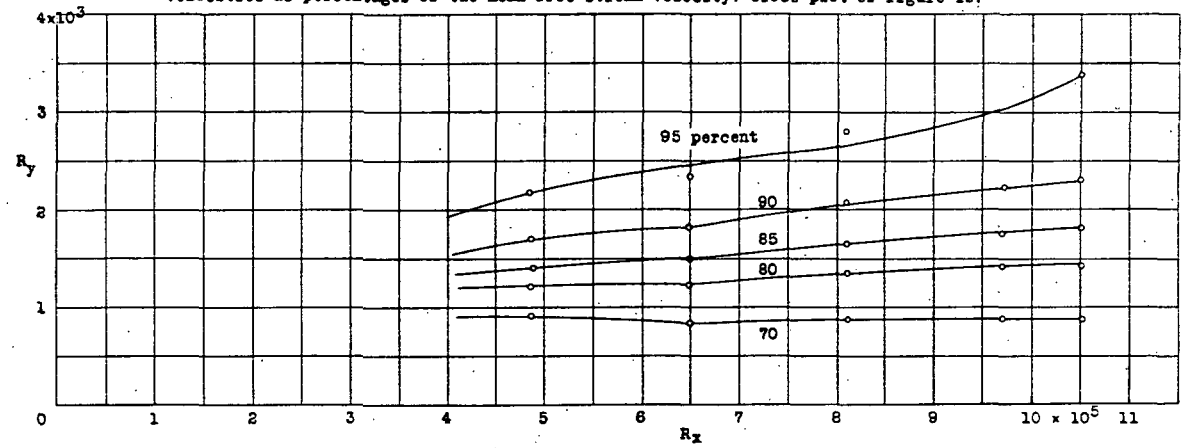

Figure 23.- Equal velocity contours at x/r = 1.348 on the convex side of the sheet. The contours give the mean velocities as percentages of the mean free-stream velocity. Cross plot of figure 16.

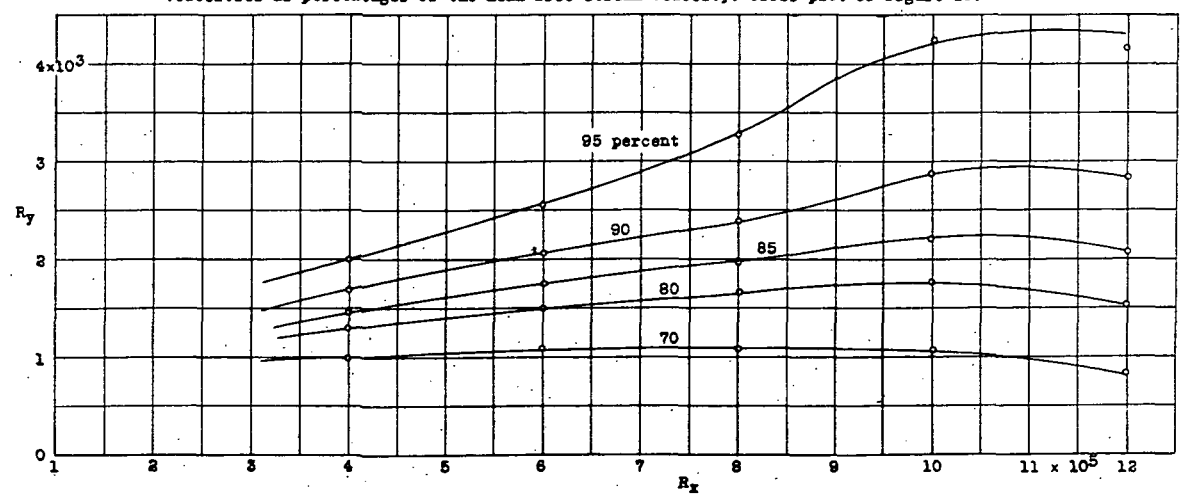

Figure 24.- Equal velocity contours at x/r = 1.652 on the convex side of the sheet. The contours give the mean velocities as percentages of the mean free-stream velocity. Cross plot of figure 17.

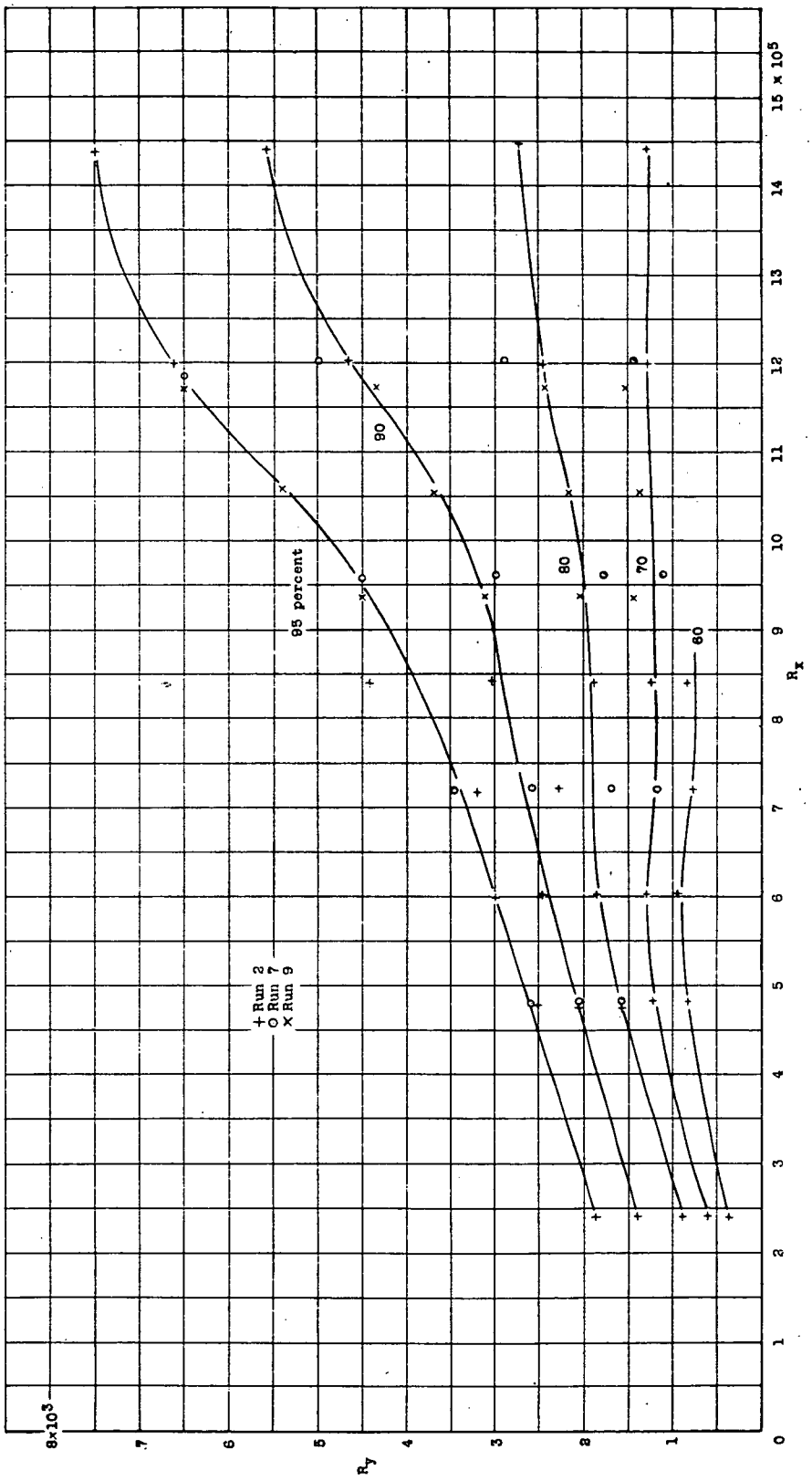

Figure 25.- Equal velocity contours at x/r = 1.975 on the convex side of the sheet. The contours give the mean velocities as percentages of the mean free-stream velocity. Cross plot of figures 18, 19, 20.

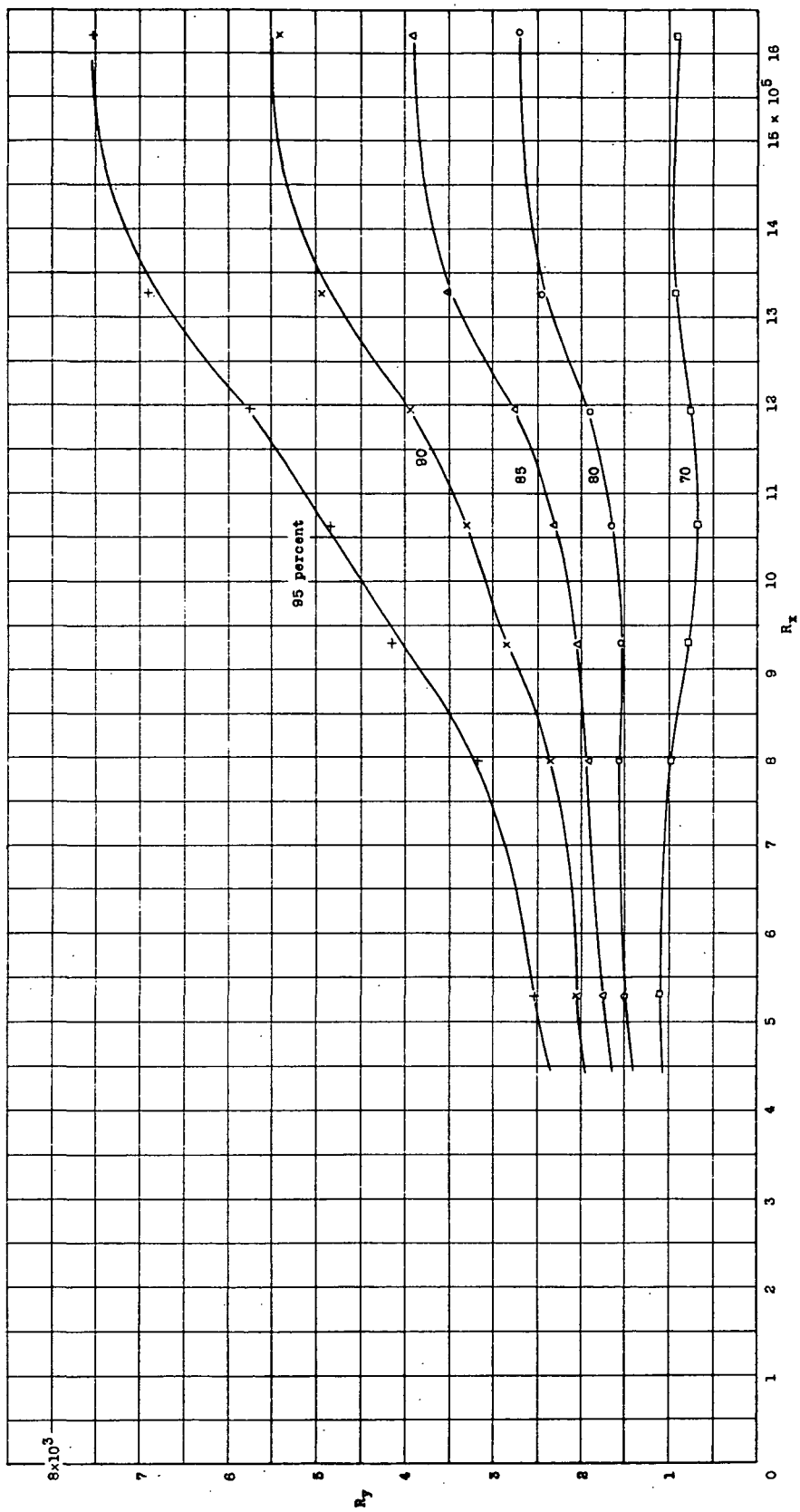

Figure 26.- Equal velocity contours at x/r = 2.250 on the convex side of the sheet. The contours give the mean velocities as percentages of the mean free-stream velocity. Cross plot of figure 21.

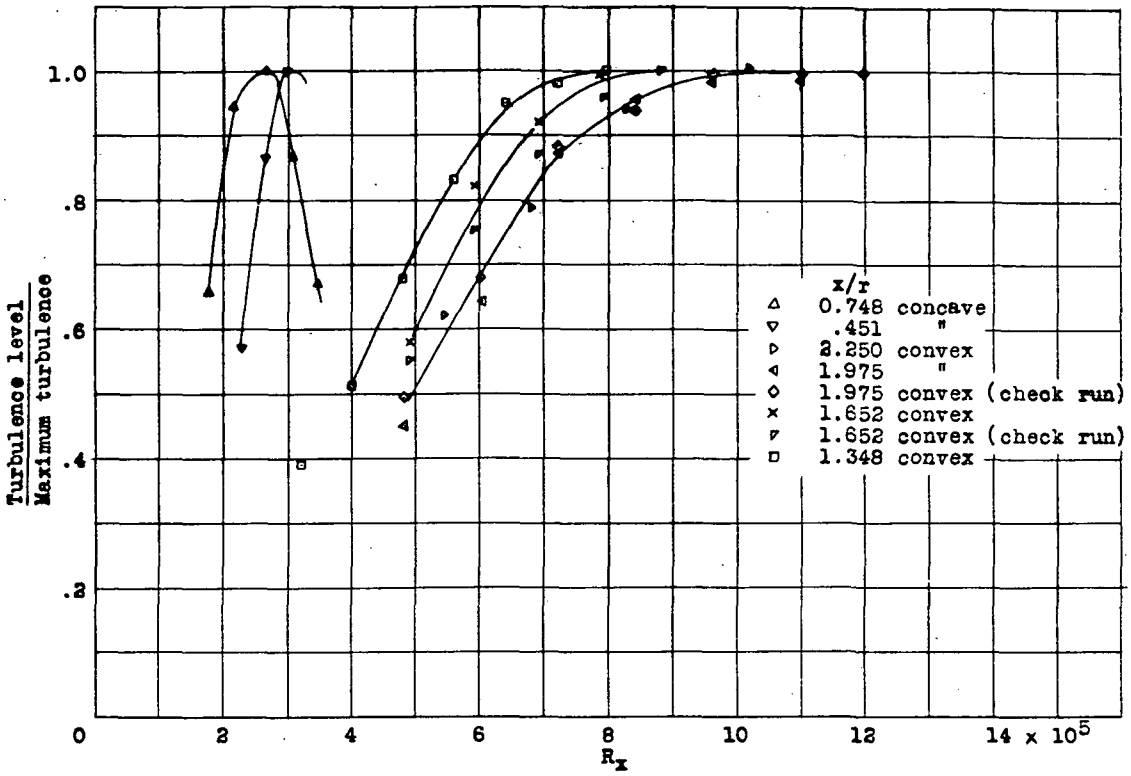

Figure 27.- Turbulence readings as function of R_x for various values of x/r.

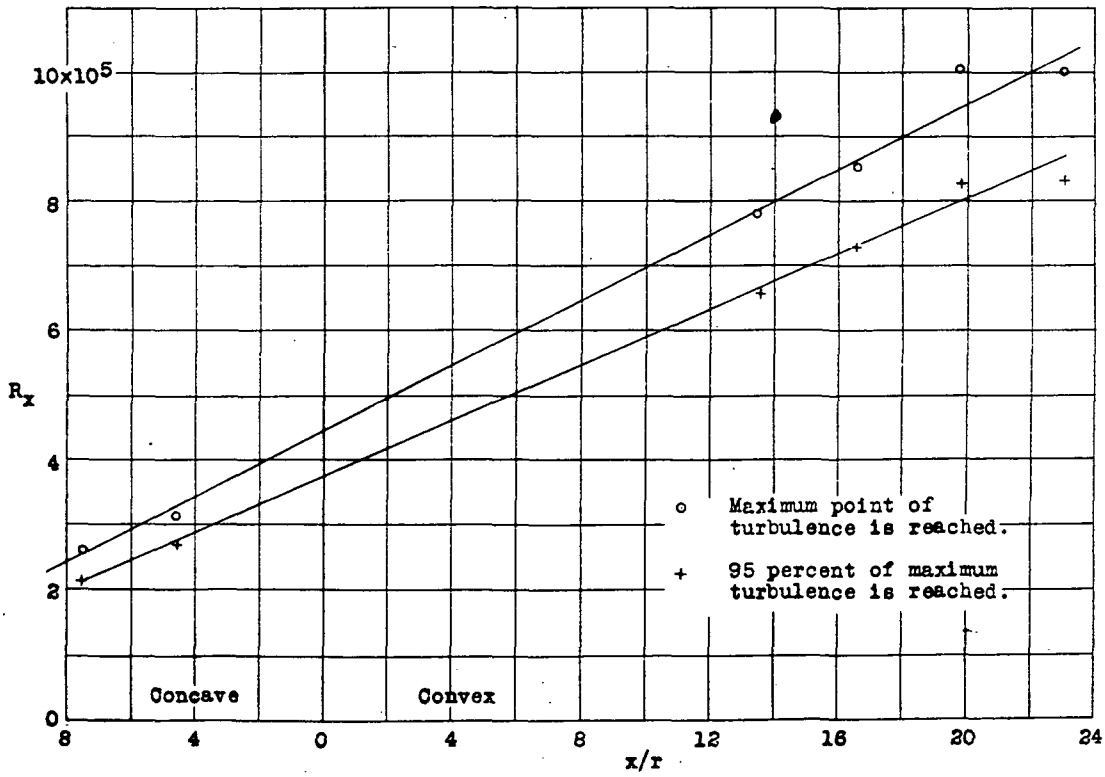

Figure 28.- Critical Reynolds Number as a function of curvature x/r.

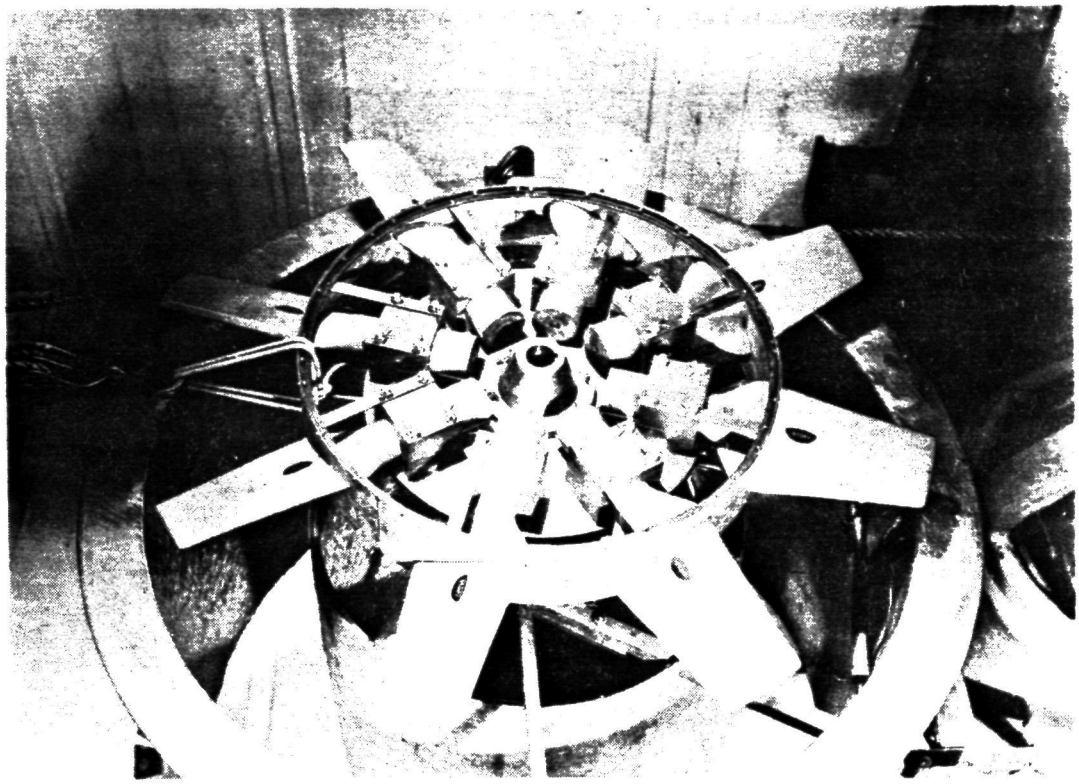

Figure 30.- Fan about to be mounted.

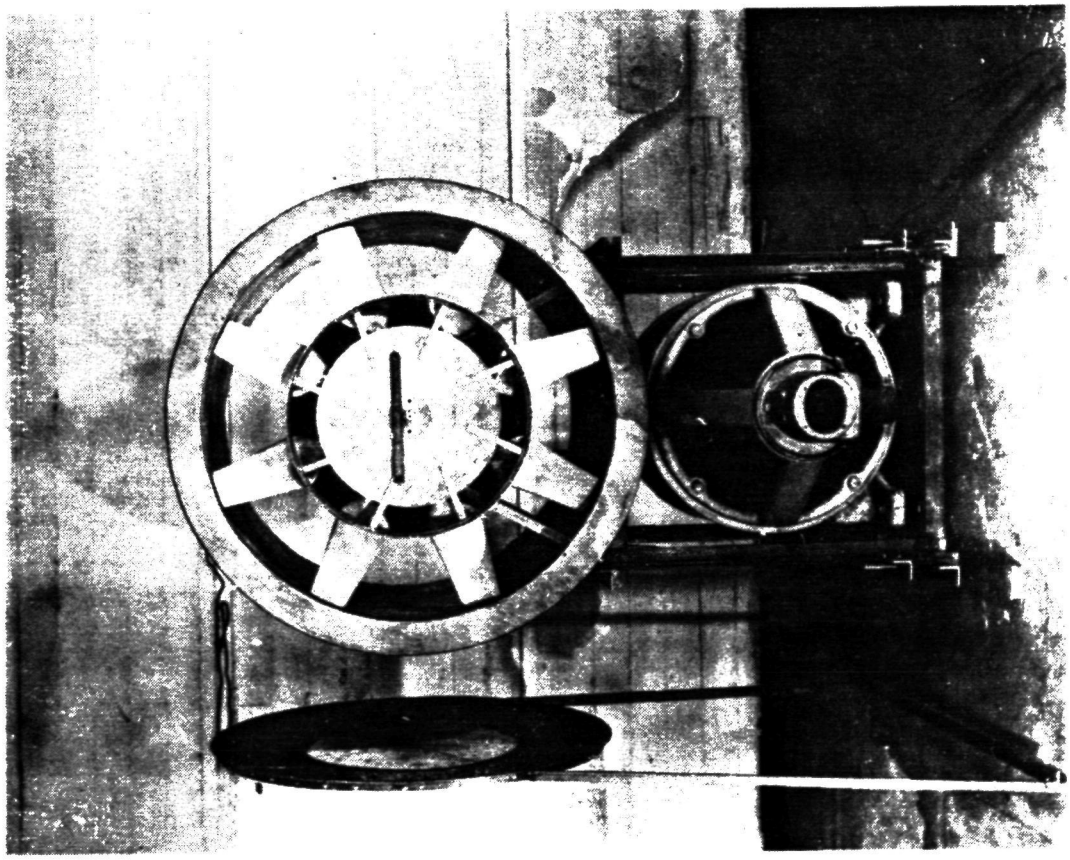

Figure 29.- Fan assembly detached from diffuser.

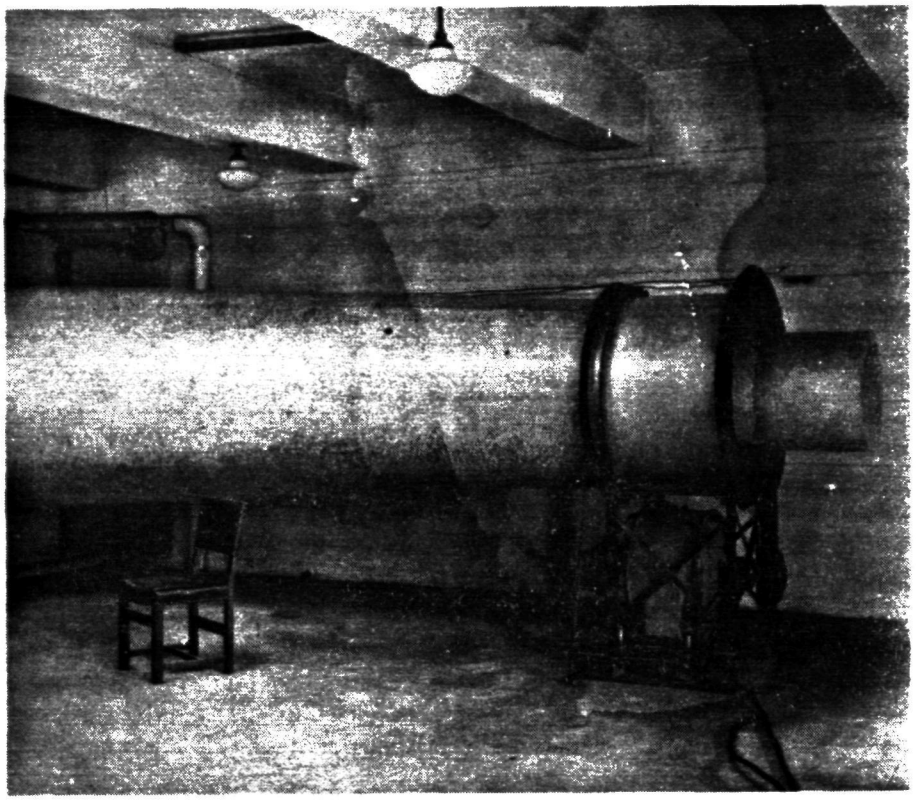

Figure 31.- Fan assembly and diffuser.

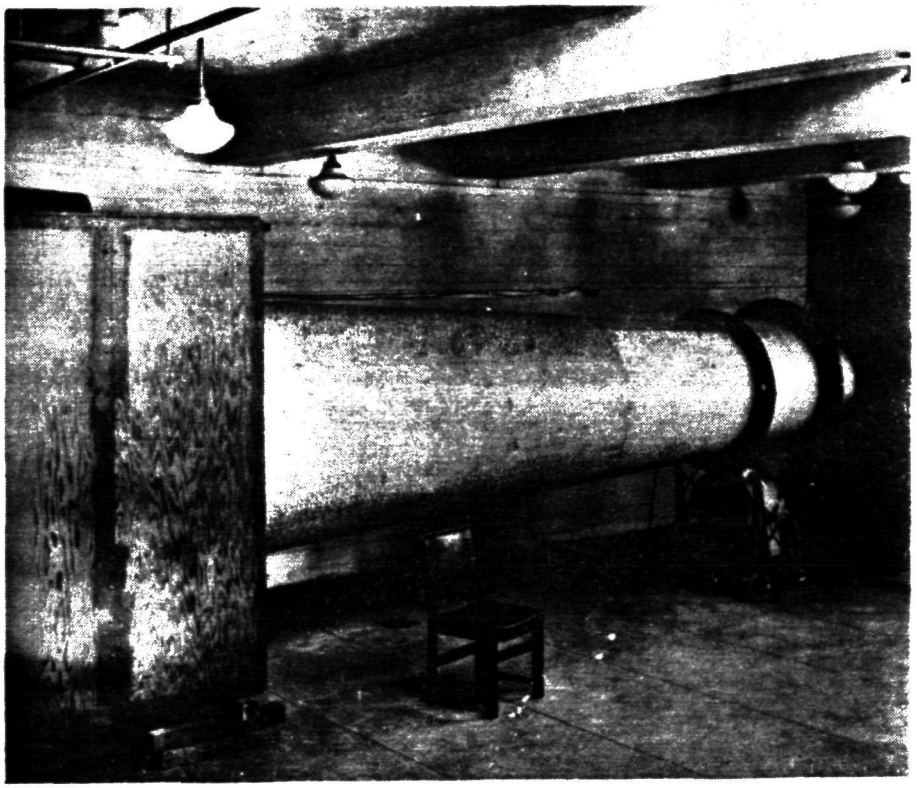

Figure 32.- Diffuser section.

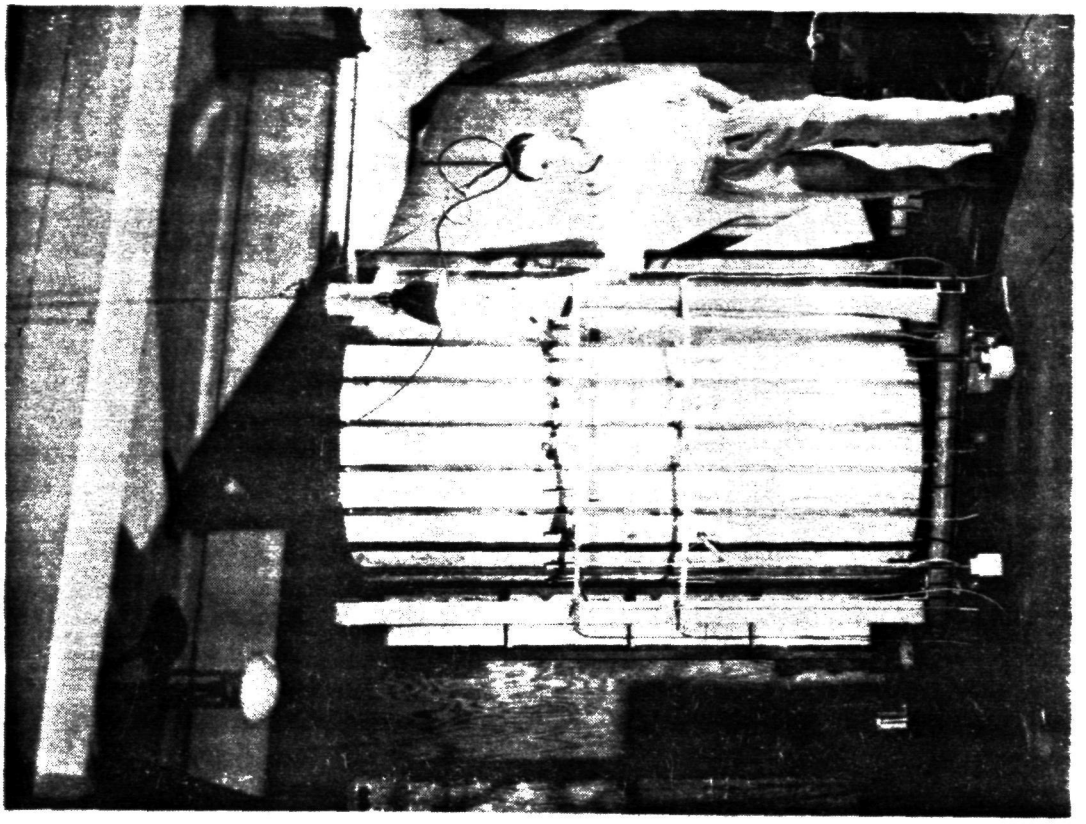

Figure 34.- The curved working section.

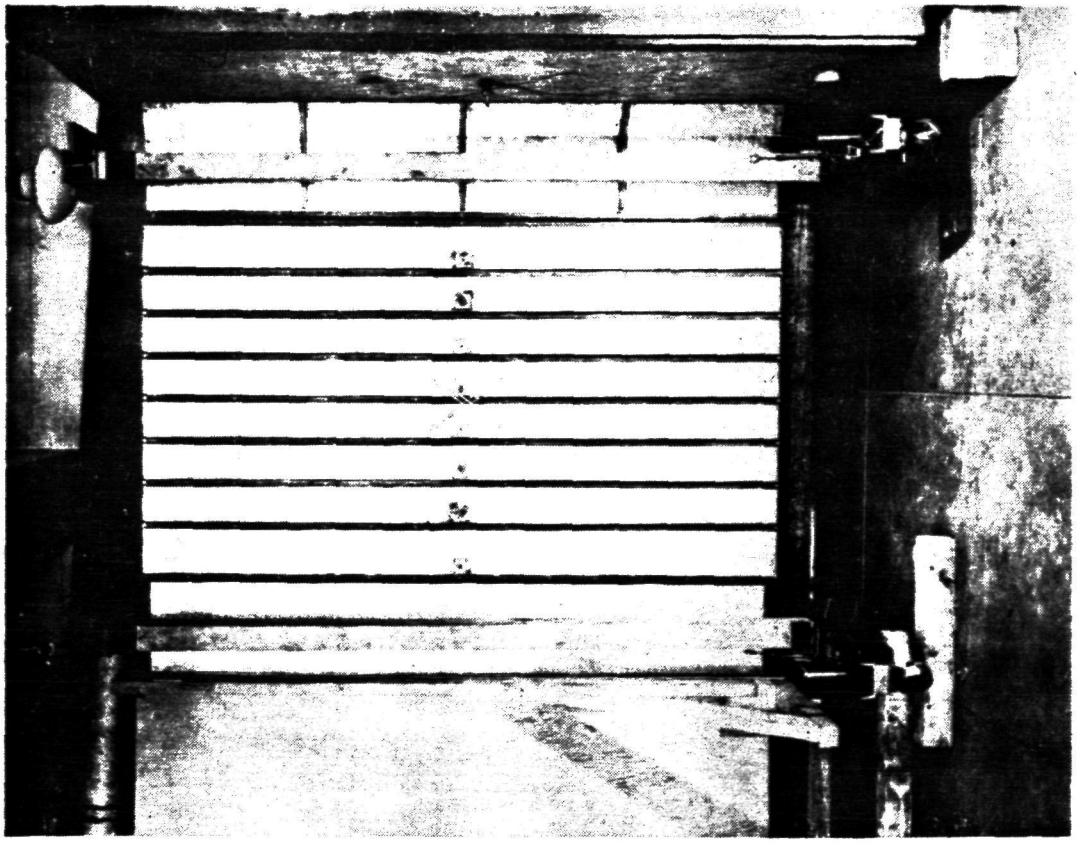

Figure 33.- The straight working section.

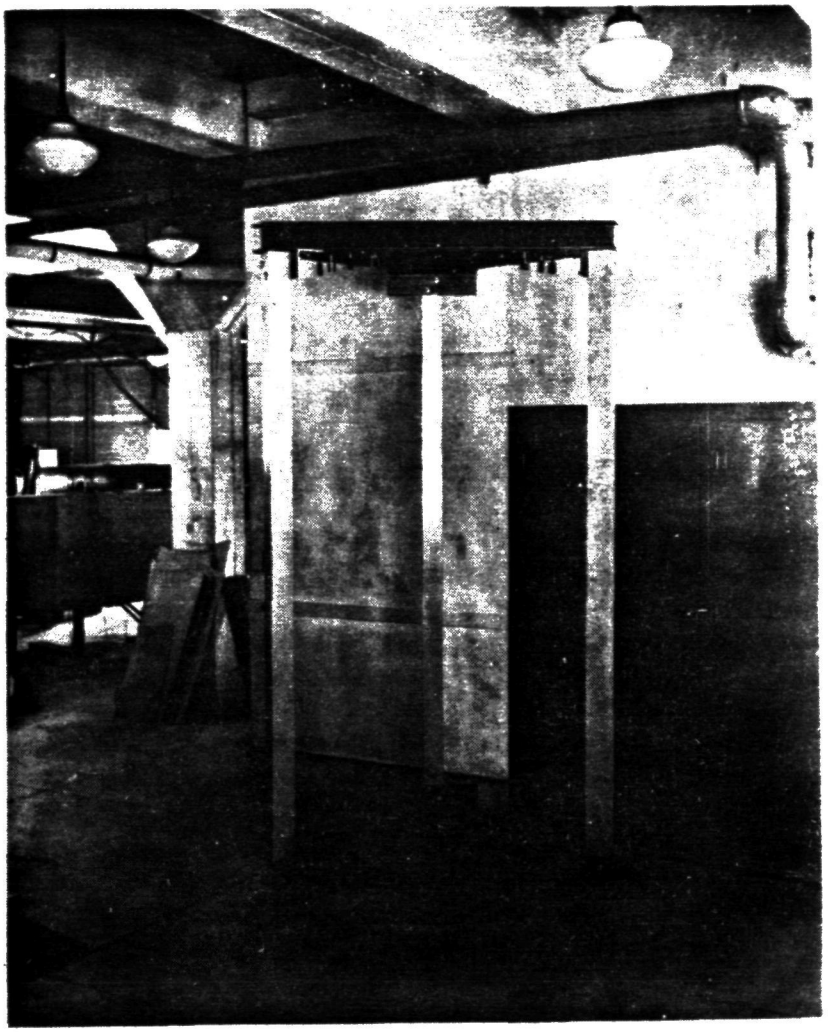

Figure 35.- The framework of the curved working section.

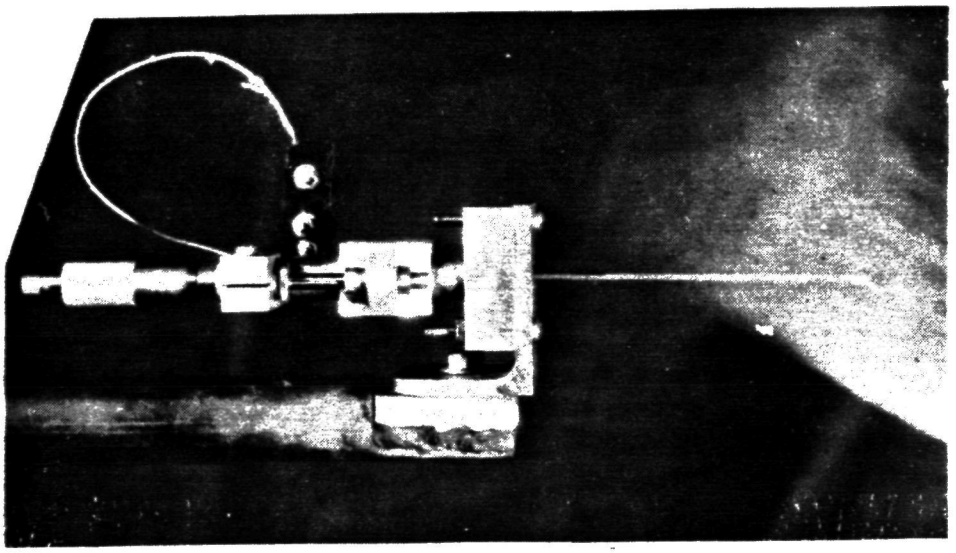

Figure 36.- Micrometer carriage hot-wire holder.

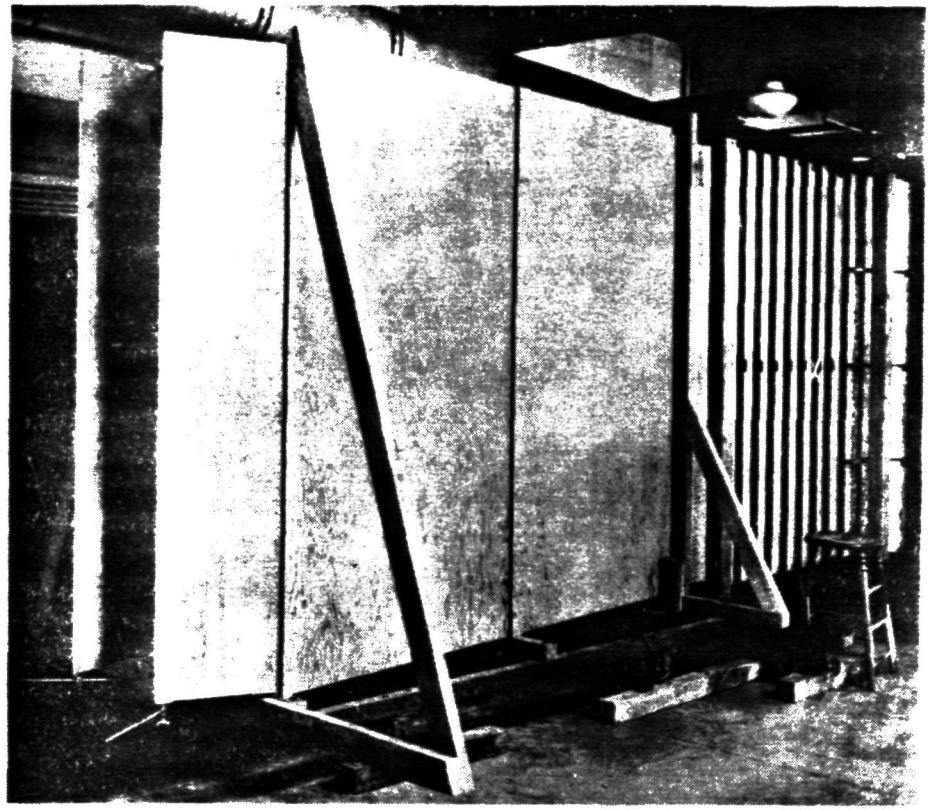

Figure 37.- Exit diffuser.

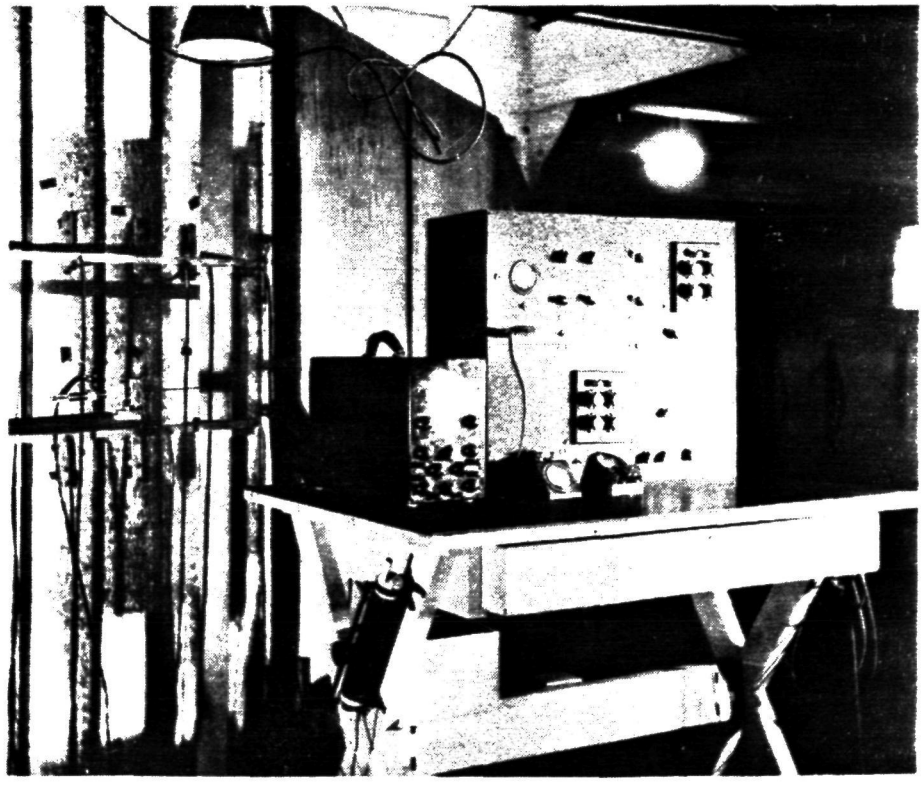

Figure 38.- The hot-wire amplifier.

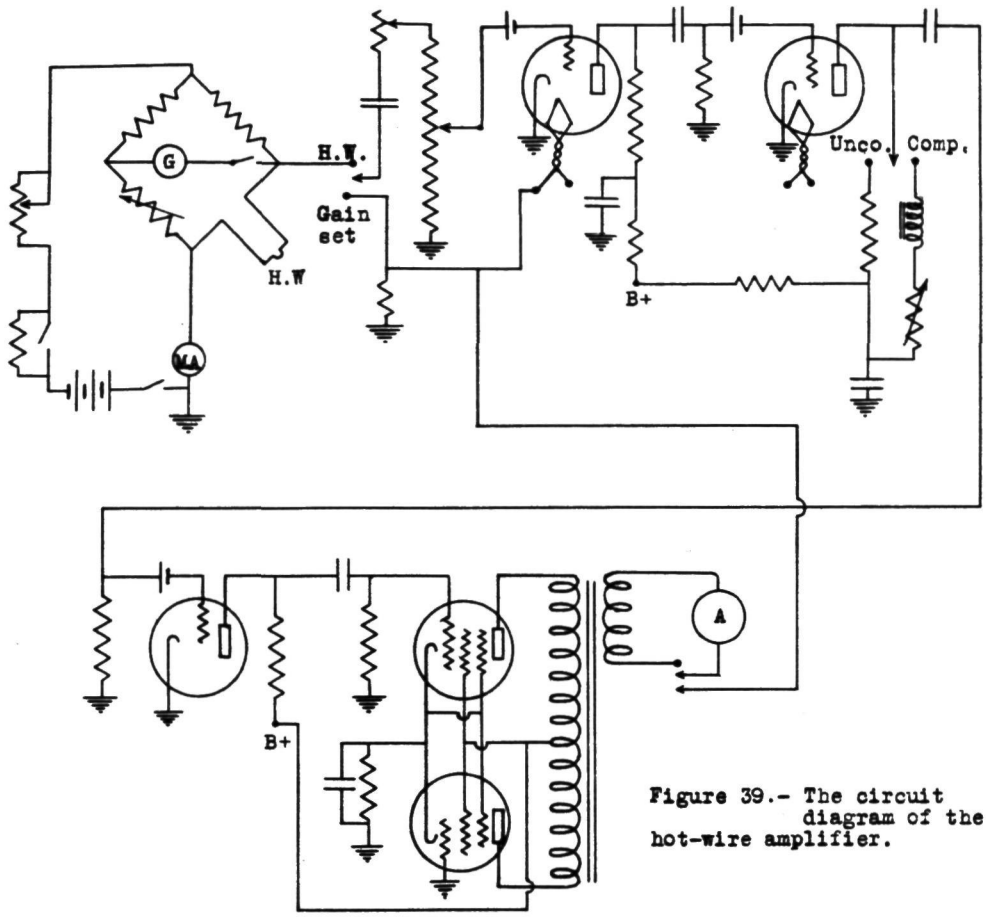

Figure 39.- The circuit diagram of the hot-wire amplifier.

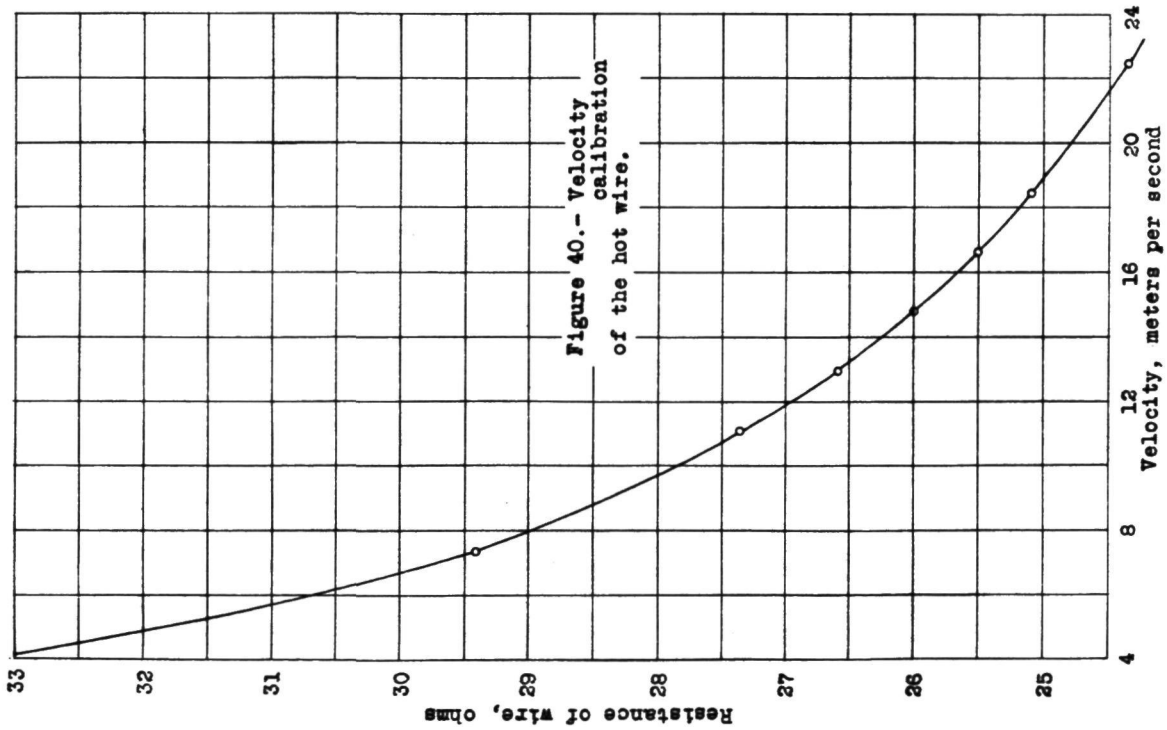

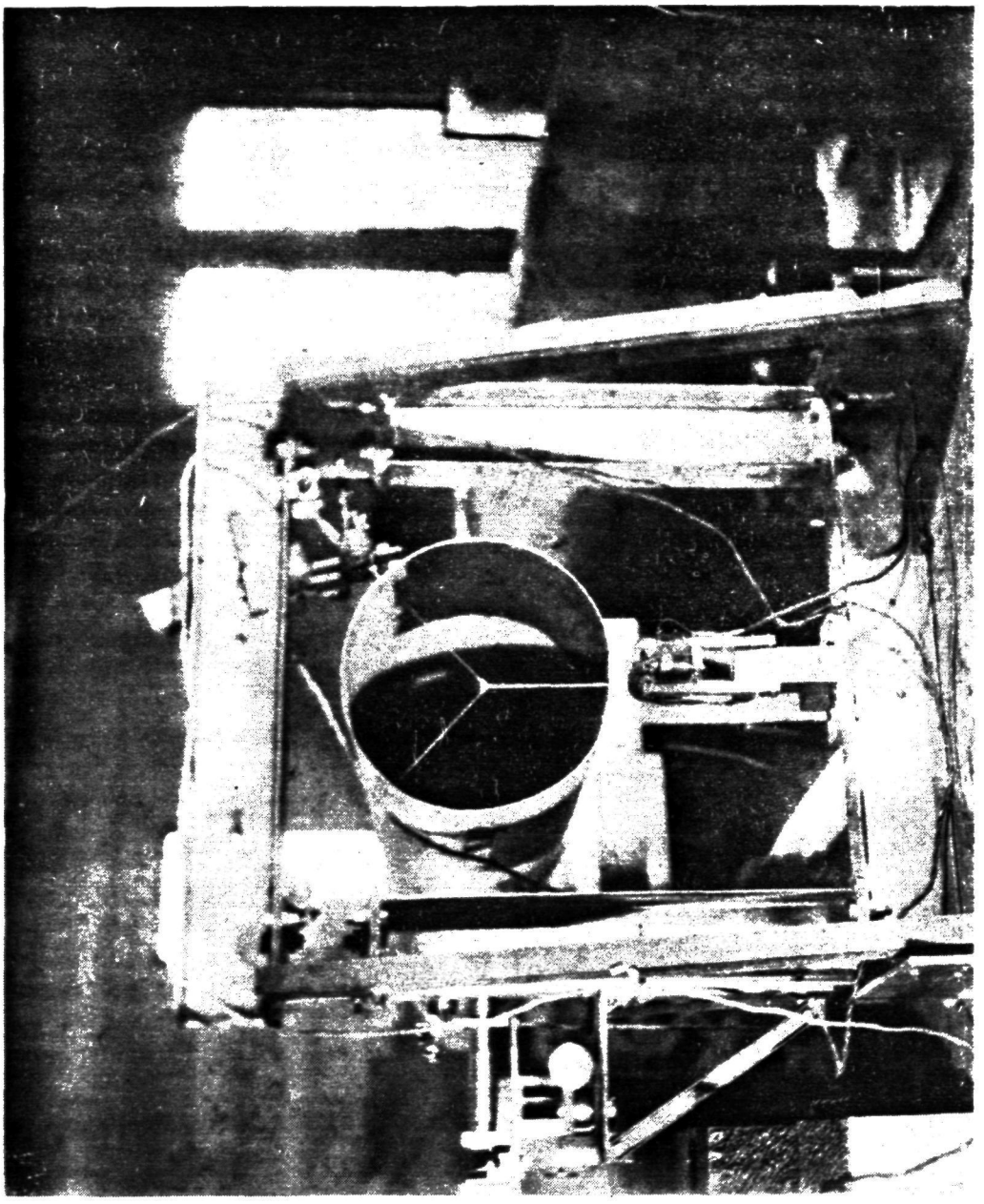

Figure 41.- Calibrating tunnel